ACS Sustainable Chemistry & Engineering

pubs.acs.org/journal/ascecg

Research Article

Sustainable Lignin Nanoparticles for Herbicide Delivery Systems: Preparation, Characterization, and Effects on Target and Nontarget Plants

Pedro H. C. de Lima, Maria C. Shiroma Buri, Rafaela S. Mendonça, Gabriel M. Favara, Érica R. Biscalchim, Mariana M. L. H. Forini, Luiz A. F. Cavalcante, and Renato Grillo*

Cite This: ACS Sustainable Chem. Eng. 2025, 13, 15460−15477

Read Online

ACCESS | Metrics & More | Article Recommendations | Supporting Information

ABSTRACT: Recent advances in nanoscience have reduced herbicide usage while maintaining crop yields, and sustainable materials, such as lignin, have emerged as promising nanocarriers for herbicide delivery. Spherical lignin nanoparticles (SLNPs) with atrazine (SLNPs_ATZ) were designed, characterized, and applied to nontarget and target plants in this work. SLNPs_ATZ displayed spherical shapes with sizes near 178 nm by dynamic light scattering (DLS), and 136 nm by nanoparticle tracking analysis (NTA), with a 74.2% loading efficiency and a 43.26% release percentage after 168 h. Chemical computational modeling revealed lower gap energies between atrazine and lignin, indicating strong carrier/bioactive interactions. Hydroponic experiments were conducted with butterhead lettuce with sublethal doses of atrazine (30 μg/L) for 28 days, and lettuce treated with SLNPs and SLNPs_ATZ showed no significant changes in root length/shoot area compared to the control. Lipid peroxidation and catalase (biochemical tests) showed significant differences between lettuce treated with atrazine and all other treatments. Gene expression of catalase-1 (CAT1) and GST6 genes indicated a possible stress tolerance in lettuce by SLNPs. Moreover, PER51 gene results indicated damage from SLNPs_ATZ and ATZ. Based on the weed control assessment, seeds/seedlings showed possible germination/development interference by SLNPs_ATZ. These findings highlight lignin as a sustainable molecule for developing nanocarriers with potential effects on gene expression and improved weed control.

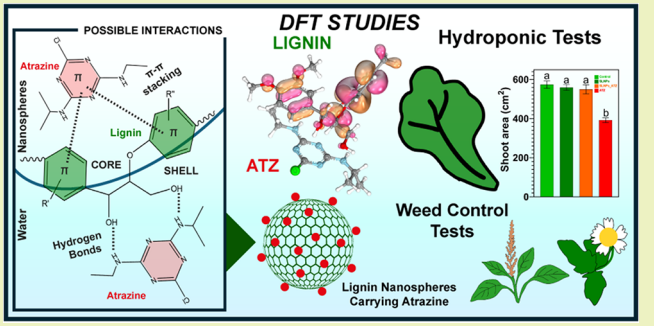

KEYWORDS: *lignin, nano-enabled agriculture, nanoherbicides, atrazine, sustainable agriculture, nontarget and target plants*

1. INTRODUCTION

The constantly growing world population has caused nations to struggle with food shortages, while farmers face crop turbulence with weed competition.[1] Weeds have developed resistance to herbicides, chemical compounds used to protect plants against them, for the last 60 years. Also, herbicides can be easily driven through leaching, drifting, or running off into the water and accidentally harming off-target plant species, animals, and humans. This highlights the need for new techniques to be developed and implemented.[2,3] Over time, the use of nano-enabled agriculture has demonstrated efficiency in delivery of herbicides (nanoherbicide) by increasing herbicidal activity and decreasing environmental impact.[4] Nanoherbicides can be derived from diverse materials (organic, inorganic, or hybrid), with organic nanomaterials being highlighted for their eco-friendly properties and effectiveness that may minimize risks to nontarget organisms and ecosystems.[5,6]

Lignin is a sustainable, natural, and organic macromolecule derived from agricultural waste. It comprises a complex phenolic structure in plant cell walls, formed by benzene units in aromatic regions and hydroxyl, carboxyl, carbonyl, and ether functional groups in aliphatic parts. This arrangement allows the formation of diverse structures (e.g., capsules, triangular, and spherical), with spherical lignin nanoparticles (SLNPs) being well known for their smooth surfaces.[7,8] SLNPs are usually prepared using the antisolvent precipitation method, where aggregation forms nanoparticles with hollows attributed to $\pi-\pi$ interactions in the benzene rings and shells formed by hydrogen bonding among carboxylic−phenolic groups in water and forming hydrophobic core/hydrophilic shell structures.[9] Recently, lignin has been explored to design nanodevices in the agricultural sector.[10] For instance, lignin-

Received: June 9, 2025
Revised: August 25, 2025
Accepted: August 26, 2025
Published: September 11, 2025

based nanoparticles can be stored for extended periods,[7] possess UV-blocking properties that may prevent active ingredients from degradation,[11] promote controlled release of active ingredients,[5,10] and lignin-composited nanocapsules have been studied as nanoherbicides.[12]

Atrazine (2-chloro-4-(ethylamino)-6-(isopropylamino)-*s*-triazine) is one of the most widely used chlorinated triazine herbicides for controlling grassy and broadleaf weeds, with 90,000 tons per year. However, it is a persistent organic contaminant with an environmental half-life of 2−57 weeks.[13] It can also have adverse effects on plants, such as growth inhibition, chlorophyll and photosynthesis reduction, and oxidative stress induction.[14] Atrazine (ATZ) has been banned in the European Union (but not in countries such as the United States and Brazil) since 2004 because its contamination and bioaccumulation affect soil and water, causing side effects on nontarget organisms.[15] Nevertheless, loading atrazine into nanocarriers may enhance its physicochemical stability and potentially reduce the required application dose.[16] However, the study of lignin nanocarrier loading of the herbicide atrazine is still scarce in the literature. For instance, previous reports (atrazine−organic compounds) demonstrated that the interactions through $\pi-\pi$ bonds with aromatic compounds (stacking) and hydrogen bonds with hydroxyls are the reason for atrazine removal in the aquatic environment. Thus, SLNPs may load bioactives through encapsulation and adsorption, incorporating ATZ (SLNPs_ATZ) due to its $\pi-\pi$ stacking and adsorbing atrazine through hydrogen bonds, providing a strong interaction.[17,18]

Nowadays, understanding how nanoherbicides behave with nontarget plants is essential to assess the risk of nano-enabled materials in agricultural products.[16,19,20] For instance, indoor hydroponics is an outstanding technique that can be used to study nanoherbicides with minimal external interference. Hydroponics has emerged as one of the most popular segments in modern controlled environment agriculture,[21] favoring overall productivity by manipulating minimum space and water, and leafy vegetables with short cultivation time, such as lettuce, have drawn attention.[22] Lettuce (*Lactuca sativa* L.) is one of the most consumed vegetables worldwide. It is easy to cultivate and is a model plant because of its sensitive response to contaminants.[23] Also, it has a higher concentration of lignin found in the cell wall of plants, providing stability and a rigid base that regulates root and leaf growth.[24,25]

To the best of our knowledge, only one study has correlated atrazine, nanoparticles, and lettuce.[15] In addition, atrazine (20 μg/L) has been reported to impact *Allium cepa*[26] and cause phytotoxicity in the macrophyte *Typha latifolia* (cattail) after 21 days in hydroponic systems.[27] Although only a few studies have considered the hydroponic systems as a means to investigate the fate and effects of nanoherbicides in plants,[28,29] this approach can be essential for supporting new findings in agro-nanotechnology. Here, lignin nanoparticles and their ability to carry atrazine herbicide were studied in a hydroponic nontarget plant species (lettuce) and target plant species *Tridax procumbens* (coat buttons) and *Amaranthus deflexus* (low amaranth) in soil. We believe this work will increase the knowledge of new nanoherbicides in modern agriculture. This research was conducted in three stages: (i) preparation and characterization of SLNPs_ATZ, (ii) impact on nontarget plants in the hydroponic system, and (iii) effects on target plants in the soil.

2. MATERIALS AND METHODS

2.1. Chemicals. Alkali lignin (AL), atrazine (purity >98%), and potassium bromide (KBr) were purchased from Sigma-Aldrich. Chloric acid (HCl), methanol, and L-methionine were purchased from Synth. Thiobarbituric acid (TBA), riboflavin, and hydrogen peroxide (H_2O_2) were purchased from êxodo. Starch and guaiacol were obtained from Dinâmica, and Flex fertilizers were obtained from Plantapar. For RT-qPCR, cetyltrimethylammonium bromide (CTAB) was purchased from Sigma-Aldrich. Primers were acquired from Exxtend Biotecnologia, DNase I (RNase Free) and Oligo DT_{12-18} primers were obtained from Thermo Fisher Scientific, and SYBR Green PCR Master Mix from Promega. *L. sativa* var. *capitata* seedlings were purchased from the domestic market. Other reagents used in laboratory preparations and procedures were of high analytical purity. Milli-Q water with a resistivity of 18.2 MΩ·cm was obtained using a Direct-Q3 UV Smart system. *T. procumbens* weed seeds were harvested on the local campus (Ilha Solteira), and *A. deflexus* seeds were purchased from Mato no Prato.

2.2. Preparation of SLNPs and SLNPs_ATZ. Lignin nanoparticles as carriers were prepared following Dai et al.'s method[30] with modifications. Briefly, 27.5 mg of alkali lignin was dissolved and magnetically stirred in 5 mL of methanol for 2 h. Later, 50 mL of water was added dropwise (at a drop rate of 82 drops per min) at room temperature (25 °C) (Figure 1A). Finally, the organic solvent was removed by rotary evaporation until 10 mL of a colloidal solution remained in water. In parallel, another solution of SLNPs with ATZ was prepared by adding 10 mg of ATZ to alkali lignin (at a final ratio of 2.75:1 (AL/ATZ, [w/w])) in methanol and following the same procedure. The final concentration of ATZ in the nanoformulation was 1 mg/mL.

2.3. Physicochemical Characterization of Nanoparticles. Ultraviolet−visible (UV−Vis) spectroscopy (Shimadzu spectrophotometer, model UV-1800) was used to study the absorption bands of SLNPs, SLNPs_ATZ, and ATZ . The spectra were collected from 200 to 800 nm.

The hydrodynamic diameter, ζ-potential, and polydispersity index of the nanoparticles were measured by dynamic light scattering (DLS) in a dilution of 200 times (Zetasizer Advance Lab (Blue Label), Malvern Instruments Ltd.; Malvern, U.K.). Also, analyses were performed to check the stability of the particles on the first day after synthesis, 7 days after synthesis, and at multiple time points up to 70 days..

Nanoparticle tracking analysis (NTA) was performed using NanoSight Pro (Malvern Instruments Ltd.; Malvern, U.K.), with a laser of 632 nm and dilution of 200 times.

Thermogravimetric analysis (TGA) was conducted using a TA Instruments SDT Q600 analyzer to evaluate the thermal stability of the nanoparticles. The test was performed under a synthetic air atmosphere from room temperature to 1000 °C at a rate of 10 °C·min^{-1}. Differential scanning calorimetry (DSC) was performed using a DSC-25 from room temperature to 200 °C at a heating rate of 10 °C/min.

Scanning electron microscopy with coupled energy-dispersive spectroscopy (SEM/EDS) was performed to observe the morphology and size distribution of the NPs. All samples were diluted 200 times and analyzed using scanning electron microscopy (SEM, EVO-LS-15, Carl Zeiss), operated at 20 kV with a spot size of 3.0−4.0 mm and a working distance (WD) of 9.5 mm.

The compounds (alkali lignin, NPs, and ATZ) were evaluated by Fourier transform infrared (FTIR) spectroscopy (Nicolet 5DXB FTIR) in the 4000−400 cm^{-1} range, using 128 scans per sample with a resolution of 4 cm^{-1} pressed into potassium bromide (KBr) pellets. All of the analyses are described in detail in Text S1.

The physicochemical stability of the nanoformulations was established by hydrogen potential (pH) using a previously calibrated pH meter (Tecnal). All data were plotted using GraphPad Prism 8.0 software.

2.4. Encapsulation Efficiency and *In Vitro* Kinetic Release Assessment. The amount of herbicide associated with nanocarriers

https://doi.org/10.1021/acssuschemeng.5c05651
ACS Sustainable Chem. Eng. 2025, 13, 15460−15477

(encapsulation efficiency) was evaluated using the ultrafiltration/centrifugation method, which involves centrifuging the nanocarrier suspension in ultrafiltration tubes composed of cellulose (Microcon, Millipore).[31] Aliquots (300 μL) were filtered by centrifugation at 3000 rpm for 10 min, and 100 μL was collected and diluted in 29.9 mL of deionized water and quantified by UV−visible spectroscopy. The encapsulation efficiency (%EE) was calculated using eq 1, where (w_f) is the final weight and (w_i) is the initial weight.

$$\%EE = \frac{w_f}{w_i} \times 100 \tag{1}$$

To assess the kinetic release profile of SLNPs_ATZ, a two-compartment model (donor−receptor) was employed, where the compartments were separated by a cellulose acetate membrane (Spectrapore, with a molecular weight cutoff of 1 kDa). 500 μL of the SLNPs_ATZ solution was placed in the donor compartment containing 49.5 mL of water. The system was gently stirred, and samples were collected over time (168 h) from the donor compartment. UV−visible spectroscopy was used to monitor the atrazine absorption peak at 222 nm. Additionally, a calibration curve previously validated by ATZ was used to quantify the release percentage.

The release data were fitted ($M_0/M_{100\%} < 0.6$) to the semiempirical Korsmeyer−Peppas kinetic model (eq 2).

$$\frac{M_0}{M_{100\%}} = Kt^n \tag{2}$$

where M_0 is the mass of atrazine released in interval t, $M_{100\%}$ corresponds to the total atrazine mass released at infinite time (100%), K is the release rate constant involving the structure and geometry of the system, t is the time, M_0 is the total mass of atrazine in time t, and n is the exponent indicative of the herbicide release mechanism, valid for Fickian and non-Fickian diffusion processes.[32]

2.5. Density Functional Theory (DFT) Studies and Chemical Reactivity. Density functional theory (DFT) studies were conducted using pre-optimized atrazine and lignin molecular structures, finding the most stable conformers using the Avogadro 1.2.0 program through random sampling with molecular mechanics techniques and considering all of the torsional angles. Since the lignin structure is large, two-dimer model compounds, 2-phenethyl phenyl ether (PPE) and bibenzyl (BB),[33] and four monomers, syringol (SYR), guaiacol (GUA), vanillyl alcohol (VAL), and vanillic acid (VAN) were used.[34] The structure of the resulting conformer was then reoptimized and obtained using the ORCA 5.0.3 program with the B3LYP\G functional and def2-TZVP basis set. Water was used as the solvent, and the images and the highest occupied molecular orbital (HOMO) and lowest unoccupied molecular orbital (LUMO) energies (in eV) were obtained in IBOview. The electronic chemical potential (μ), chemical hardness (η), chemical softness (S), and electrophilicity index (ω) were calculated using LUMO and HOMO results, according to Belakhdar et al.[35]

2.6. Effects on Nontarget Organism. *2.6.1. Lettuce in Hydroponic Treatments and Morphological Assessments.* Sixty-four butterhead lettuce (*L. sativa* var. *capitata*) seedlings were acclimated for 1 week in fertilized water at 16−26 °C (under controlled environmental conditions) in a hydroponic system. Two types of fertilizers were used in the hydroponic system in water: blue and red at a ration of 1:1.048 (w/w), and the compounds of the fertilizers are listed in Tables S1 and S2. Then, 16 seedlings for each treatment (Control, SLNPs, SLNPs_ATZ, and ATZ) were separated. After 7 days, 27 mL of an ATZ stock solution (10 mg/L) was added to the tank, followed by fertilized water until a 9 L point was reached, resulting in a 30 μg/L concentration. Then, 270 μL of SLNPS_ATZ solutions (atrazine concentration: 1 mg/mL) was placed in their respective tanks, with a total atrazine quantity of 270 μg in ATZ and SLNPs_ATZ solutions (or 16.875 μg per lettuce). The same amount (270 μL) of SLNPs was used, and the control was kept only in fertilized water. The length and area of the lettuce shoots and roots were measured on days 0, 14, and 28. The width and area of the leaves were measured on day 28. All measurements were taken using ImageJ based on photos of the lettuce leaves.

2.6.2. Chlorophyll and Carotenoid Contents. Chlorophyll *a*, *b*, and total were measured using a nondestructive assay, enabling continuous observation. Lettuce was analyzed on days 0, 14, and 28 using a digital chlorophyll content meter (clorofiLOG, FALKER) and measured in the Falker chlorophyll index (FCI). Carotenoids were calculated according to Ng et al.[36] using eqs 3−5. After 28 days, 100 mg of lettuce leaves were macerated with 6 mL of pure methanol, the solution was centrifuged at 3000 rpm for 10 min, and 2 mL was analyzed using a spectrophotometer.

$$C_a\left(\frac{\mu g}{mL}\right) = 16.72A_{665} - 9.16A_{652} \tag{3}$$

$$C_b\left(\frac{\mu g}{mL}\right) = 34.09A_{652} - 9.16A_{665} \tag{4}$$

$$C_{(x+c)}\left(\frac{\mu g}{mL}\right) = (1000A_{470} - 1.63C_a - 9.16C_b)/221 \tag{5}$$

2.6.3. Starch Concentration Levels. Starch concentration levels (mg/mL) were calculated after 28 days according to Rawashdeh et al. and Antunes et al., with modifications.[37,38] Lettuce samples (1 g) were soaked in sodium phosphate buffer and incubated at 37 °C for 10 min. Next, a solution of soluble starch (1% w/v) was added, and the mixture was mixed and incubated at 37 °C for 15 min. HCl was added to stop the reaction, followed by iodine reagent (potassium iodide[KI] and iodine [I_2]). Absorbance was measured at 620 nm using a spectrophotometer, and a standard calibration curve previously validated with five different concentrations was used to calculate the final concentration.[38]

2.6.4. Lipid Peroxidation. Malondialdehyde (MDA) content was determined following the methods of Wang et al. and Behtash et al.[39,40] After 28 days, lettuce roots and leaves (1 g) were crushed using a mortar and pestle in 5 mL of 10% trichloroacetic acid. After 3 min of centrifugation, 2 mL of the supernatant was mixed with 2 mL of 0.67% thiobarbituric acid. The reaction mixture was placed in a water bath at 95 °C for 30 min, then cooled on ice, and centrifuged for 3 min. The absorbance of the supernatant was measured at 450, 532, and 600 nm. The MDA content was calculated using eqs 6 and 7, where w is the weight of the sample.

$$\text{MDA concentration}\left(\frac{\mu mol}{L}\right) = 6.45(A_{532} - A_{600}) - 0.56A_{450} \tag{6}$$

$$\text{MDA content}\left(\frac{\mu mol}{g\ FW}\right) = \text{MDA concentration} \times 5/m \tag{7}$$

In addition, other aldehydes (1-hexanal, 1-butanal, 1-propanal, and 1-propanaldehyde methyl acetal) were measured according to Fotovvat et al.,[41] by calculating the absorption at 455 nm using an extinction coefficient of 0.457×10^{-5} M cm^{-1}.

2.6.5. Peroxidase, Catalase, and Superoxide Dismutase Activity. Enzyme extraction was performed as described by Azevedo et al. with modifications,[42] where 2.5 g of leaves and roots (after 28 days) were macerated with 10 mL of refrigerated extraction formed by 3 mM of dithiothreitol (DTT) and 1 mM ethylenediamine tetraacetic acid (EDTA) in a phosphate buffer (pH 7.0) with 4% (w/v) polyvinylpyrrolidone. Then, the homogenate was centrifuged at 10,000 rpm and 4 °C for 20 min.

Guaiacol peroxidase (POD) activity was measured by adding 90 μL of the extract, 2 mL of phosphate buffer (pH 7.0), 200 μL of 1% (v/v) guaiacol, and 100 μL of 0.16% (v/v) H_2O_2. The absorbance was measured at 470 nm using a spectrophotometer after 1 min. The POD activity was calculated using a molar extinction coefficient of 2.47 mM^{-1} cm^{-1}, and the enzyme activity was expressed as nmol H_2O_2 oxidized min^{-1} g^{-1} FW. Catalase (CAT) activity was determined using a reaction mixture containing 3 mL of 12.5 mM H_2O_2 in phosphate buffer (pH 7.0) and 100 μL of the extract. The

https://doi.org/10.1021/acssuschemeng.5c05651
ACS Sustainable Chem. Eng. 2025, 13, 15460−15477

decrease in absorbance was measured at 240 nm with a gap of 2 min, and CAT activity was calculated using a molar extinction coefficient of 39.4 mM^{-1} cm^{-1} and expressed as nmol H_2O_2 decomposed min^{-1} g^{-1} FW. The enzyme contents of POD and CAT were determined according to Chance and Maehly.[43]

Superoxide dismutase (SOD) activity was determined according to Silva Santos et al., with modifications.[44] Briefly, 50 μL of the extract was mixed with 2 mL of a larger solution containing 9.6 mL of phosphate buffer (pH 7.0), 6 mL of nitro blue tetrazolium (NBT) (0.44 mM), 6 mL of L-methionine (6.5 mM), 2.4 mL of 1 mM riboflavin, and 6 mL of EDTA (50 nM), totaling to 30 mL. The mixture was then exposed to fluorescent light (20 W) at 25 °C for 15 min, while the control was kept in the dark. The SOD activity was measured at 560 nm using a spectrophotometer, with the SOD activity defined as the difference in the absorbance of illuminated and non-illuminated samples. The results were expressed in units of SOD (U) g^{-1} FW.

2.6.6. FTIR Spectroscopy of Lettuce. Briefly, after 28 days, the samples of the four types (control, SLNPs, SLNPs_ATZ, and ATZ) of lettuce leaves and roots were placed in a oven at 37 °C for 4 days. Then, 10 mg of samples were mixed with 140 mg of KBr, ground, compressed, and analyzed by FTIR spectroscopy. Finally, the second derivation was analyzed by plotting the data using GraphPad Prism 8.0.

2.6.7. Gene Expression Analysis. 2.6.7.1. Total RNA Extraction. Six plants per treatment were randomly selected for leaf and root sampling for total RNA extraction. From each plant, 100 mg of root tissue was weighed, and 1.2 cm diameter discs were collected from three distinct leaf sections: the base, center, and margin. RNA extraction was performed according to Doyle and Doyle.[45] In this method, leaf and root tissues were crushed in 400 μL of cetyltrimethylammonium bromide (CTAB) extraction buffer and incubated for 30 min at 65 °C. Subsequently, 400 μL of chloroform was added, followed by vortexing for 1 min, and centrifugation at 13,000 rpm for 5 min. The supernatant (approximately 200 μL) was transferred to a new microcentrifuge tube, and 200 μL of isopropanol was added, mixed, and incubated at −20 °C for 1 h. The samples were centrifuged at 13,000 rpm for 5 min at 4 °C, the supernatant was discarded, and the pellet was washed with 200 μL of 70% ethanol at 13,000 rpm for 5 min. The supernatant was discarded, and the pellet was dried. Finally, the pellet was resuspended in 50 μL of nuclease-free water, treated with DNase, and the extracted RNA was stored in an ultrafreezer at −80 °C.

2.6.7.2. cDNA Synthesis and qPCR Gene Amplification. RT-qPCR was used to identify oxidative stress gene expression levels using a real-time PCR system (BioRad). GAPDH, PER551, catalase1 (CAT1), and GST6 gene expression levels (Table 1)[46−48] were measured using the GoTaq 1-Step RT-qPCR System (Promega). In a total volume of 10 μL, the reactions were performed using 2 μL (50 ng/μL) of RNA, 5 μL of GoTaq qPCR Master Mix, 2×, 2.5 μL of ultrapure water, 0.1 μL of GoScriptRT (Promega), and 0.2 μL of each primer pair at a concentration of 10 μM. In a thermocycler, the reactions were carried out at 37 °C for 30 min, and the initial denaturation was held at 95 °C for 10 min, followed by 40 cycles of denaturation at 95 °C for 10 s, annealing, and extension at 60 °C for 30 s. The final melting temperature step was set at 65−95 °C for 0.5 s. Real-time PCR efficiencies were obtained using the LinRegPCR software, version 2021.2. Glyceraldehyde 3-phosphate dehydrogenase (GAPDH) was used as the reference gene. The relative expression level was calculated using the $2^{-\Delta\Delta CT}$ method (Livak et al.).[49]

Table 1. Primers Selected for Gene Expression Analysis

name of the gene	primer sequences (5′− 3′)
CAT1	5′-GGTCCAAGGCGATGTCTTTG-3′
	5′-ATGAACAGCTGGCGTTTTGT-3′
PER51	5′-CTGTCAACACATGGGCTTCC-3′
	5′-TCCCACTTCGACCCGTTTTA-3′
GST6	5′-GCCCAAATACTTGCTCTCCG-3′
	5′-TTGGGATGACTACCGACGAG-3′
GAPDH	5′-AGGTAGCGATCAACGGATTC-3′
	5′-AGGTGGGATGCTTGTTTGAC-3′

2.7. Effect of Target Organism in Sublethal Doses, Chlorophyll, and Fresh Weight. Ten seeds of *T. procumbens* and *A. deflexus* were sown in thirty-two pots (each species) in a greenhouse under mild conditions (maximum temperature: 28 °C and three times of irrigation) per 1 day. Four treatments were predetermined: Control, SLNPs, SLNPs_ATZ, and ATZ, each with octuplicate repetitions (n = 8). The soil utilized was Carolina soil (sterilized soil, free from microbes and pH 5.5). The experiment continued to have three irrigation per day to maintain humidity and was monitored using a humidity meter (40−100% humidity). For preemergence treatment, ATZ and SLNPs_ATZ were applied at 44 g of active ingredient per hectare (44 g a.i. ha^{-1}). Then, 27 mL of ATZ solution (10 mg/L) and 270 μL of SLNPs_ATZ (1 mg/mL of atrazine) were combined in Erlenmeyer flasks and then filled with purified water until 80 mL (for each weed) was reached. Then, 10 mL was used for each pot, resulting in a total of 16,875 μg per pot (same quantity per lettuce) or 44 g a.i. ha^{-1}. Moreover, 270 μL of SLNPs (same quantity in hydroponics) and control (no treatment) were used. Sublethal doses were used to facilitate the observation of differences between treatments since higher doses would cause total crop mortality. Photos were taken on days 4, 8, 14, and 28 for *T. procumbens*, while additional photos were taken for *A. deflexus* on days 11 and 21. Germination rates were measured until day 14 for *T. procumbens* and day 21 for *A. deflexus*. Fresh weight and survival rate were measured after 28 days, and chlorophyll levels were measured only in *T. procumbens* seedlings due to the small leaf size.

3. RESULTS AND DISCUSSION

3.1. Physicochemical Characterization of the Nanoparticles. Lignin has a unique structure with hydroxyl and benzene rings in abundance. The use of this biomolecule to fabricate nanoparticles may be achieved through the simple procedure of antisolvent precipitation. During the process, lignin dissolves in the solvent (methanol in our case) and forms spherical particles in contact with water (antisolvent); it is believed that the structure can self-assemble due to H-bonding (shaping the surface) and $\pi-\pi$ stacking in the core.[50,51] Through all forms of carrying a bioactive compound by nanoparticles, two ways in which SLNPs can carry ATZ can be hypothesized in this work: surface and cavity loading.[18] In our experiment, atrazine was mixed with alkali lignin in methanol, and during this time, two possible interactions (Figure 1A) may be observed: hydrogen bonding between lignin hydroxyls and atrazine amines and $\pi-\pi$ stacking among the aromatic structures. These schematic interactions are shown for other molecules with a similar form to lignin (with benzene rings and hydroxyls) and ATZ; in their cases, the organic compound was used to remove atrazine.[17,52,53] In our case, since atrazine was combined with lignin, it is possible that part of the atrazine was carried inside the nanoparticle cavities and part was adsorbed by the SLNP surfaces during antisolvent precipitation. However, the mechanism needs to be studied in the future.

The integrity of the spherical morphologies was observed, and nanoparticles with good dispersion were observed in the SEM images of both SLNPs and SLNPs_ATZ (Figure 1B-1,B-2). In addition, the relative percentage frequency distribution (%) of the nanoparticles with and without atrazine was plotted, and it was noticed that SLNP (Figure S1A) sizes ranged between 140 and 150 nm. This method with methanol presented a smaller size compared to other solvents such as tetrahydrofuran (THF), where spherical nanoparticles ranged

https://doi.org/10.1021/acssuschemeng.5c05651
ACS Sustainable Chem. Eng. 2025, 13, 15460−15477

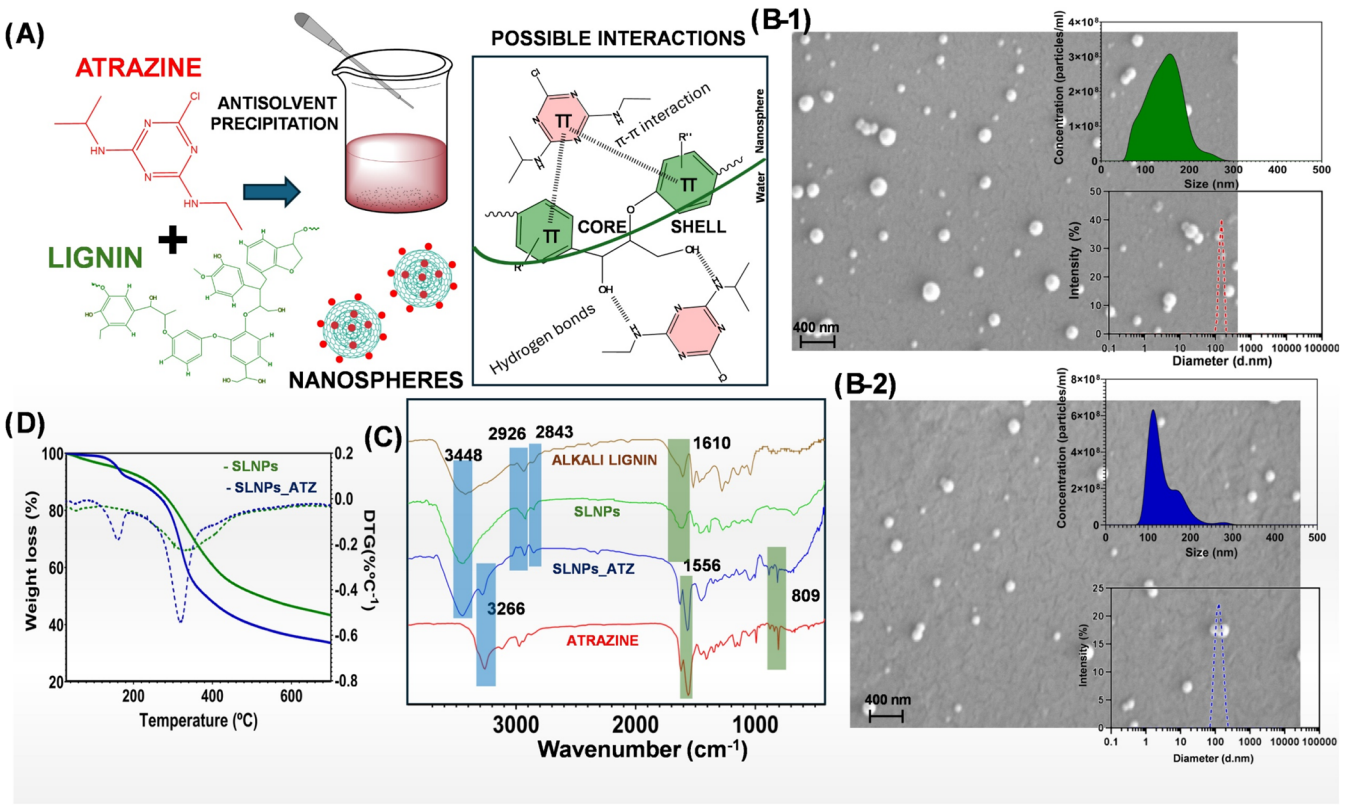

Figure 1. (A) Preparation of spherical lignin nanoparticles loaded with atrazine and their possible interactions; (B-1, B-2) scanning electron microscopy (SEM), dynamic light scattering (DLS), and nanoparticle tracking analysis (NTA) results of SLNPs and SLNPs_ATZ; (C) Fourier transform infrared (FTIR) spectra of alkali lignin, SLNPs, SLNPs_ATZ, and ATZ; and (D) thermogravimetric analysis (TGA) of SLNPs and SLNPs_ATZ.

from 250−350 nm.[54,55] Moreover, nanoparticles with atrazine and SLNPs_ATZ (Figure S1B) had higher peaks around 110−120 nm. Subsequently, DLS and NTA of SLNPs (Figure 1B-1) analyses were performed, and by DLS, the nanoparticles had a size of around 160 nm (mean: 161.4 ± 1.93 nm). By NTA, they presented similar results (with a mean of 145 ± 45 nm), where the partial percentages were 6.12% in the range of 20−80 nm, 87.28% in 81−205 nm, and 5.87% 206−300 nm. The SLNP size of around 145 ± 45 nm is close to the value obtained by Dai et al., where they found sizes of 131.2 nm. Moreover, SLNPs_ATZ (Figure 1B-2) showed a range around 154−203 nm (with a mean of 178.6 ± 24.7 nm) by DLS, although they were slightly lower in NTA analyses (with a mean of 136 ± 43 nm): 1.57%(251−350 nm), 25.61% (151−250 nm), and 72.1% (60−150 nm).[30]

The FTIR spectrum of pure atrazine (Figure 1C) indicated N−H stretching at 3266 cm^{-1}, deformation of the triazine group at 1556 cm^{-1}, and C−Cl stretching at 809 cm^{-1}. All of the previous peaks matched the SLNPs_ATZ FTIR, suggesting the presence of pure atrazine outside the nanoparticles, which may be correlated with the adsorption of the herbicide by SLNPs.[56] The hydroxyls of the lignin phenolic groups are observed at 3448 cm^{-1} in SLNPs_ATZ, SLNPs, and alkali lignin (AL).[57] Also, all lignostructures presented bands at 2926 and 2850 cm^{-1}, resulting from the symmetrical and asymmetrical C−H stretchings vibrations of the methyl and methylene groups. Nonetheless, only AL and SLNPs showed bands around 1610 cm^{-1}, which are related to the aromatic skeletal vibrations of lignin.[58]

Also, a peak was observed at 275 nm by UV−visible spectroscopy analysis (Figure S1C), which is characteristic of spherical lignin nanoparticles.[59] In addition, TGA analysis (Figure 1D) showed thermal differences between SLNPs and SLNPs_ATZ. The TGA curve of SLNPs_ATZ exhibited a variation at around 190 °C compared to that of SLNPs, which can be correlated to the melting temperature (T_m) of free ATZ (around 175 °C), which is not encapsulated.[60] This slight increase in T_m may be due to a possible strong hydrogen bond interaction between the lignin and atrazine. Also, the TGA of the lignin nanoparticles exhibited a behavior similar to what has been reported in the literature. Rapid weight loss was readily observed at 100 °C for SLNPs, indicating that the water molecules were captured by the hydrophilic groups of SLNPs. A rapid decline in weight loss between 200 and 450 °C was correlated with interunit linkages such as aryl ether bond (such as β-O-4) linkages that started to pyrolyze and may have led to lignin oxidation. The aromatic rings (strong C−C bonds) slowly decomposed above 500 °C. Finally, the char residue was observed at 700 °C.[61,62]

By DSC analysis (Figure S2A), the glass transition (T_g) of SLNPs was observed at around 120 °C, but the T_g of lignin can reach 160 °C.[63] In Figure S2B, the T_m of ATZ in DSC is corroborated with the TGA curve. For example, Gautam et al. showed only a peak of ATZ at around 181 °C, which correlated with the T_m of the compound. Since SLNP_ATZ presented another peak at around 95 °C,[64] this may indicate a shift of the SLNP peak (decrease of T_g), which may confirm the theorization discussed above. Part of the herbicide was outside the nanoparticles (interacting via hydrogen bond

https://doi.org/10.1021/acssuschemeng.5c05651
ACS Sustainable Chem. Eng. 2025, 13, 15460−15477

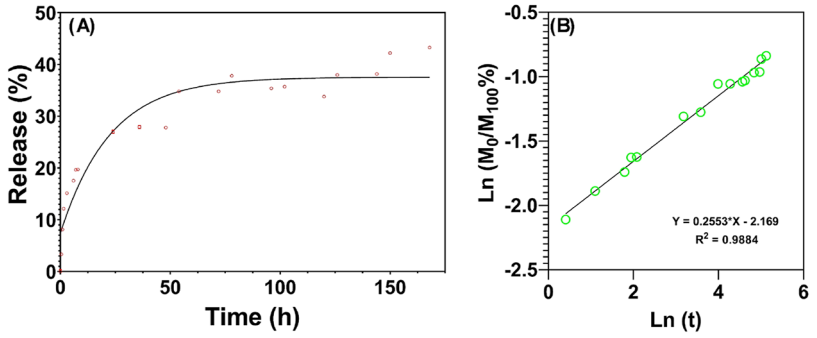

Figure 2. (A) Release curve of spherical lignin nanoparticles containing atrazine. (B) Release data fitted to the Korsmeyer−Peppas kinetic model.

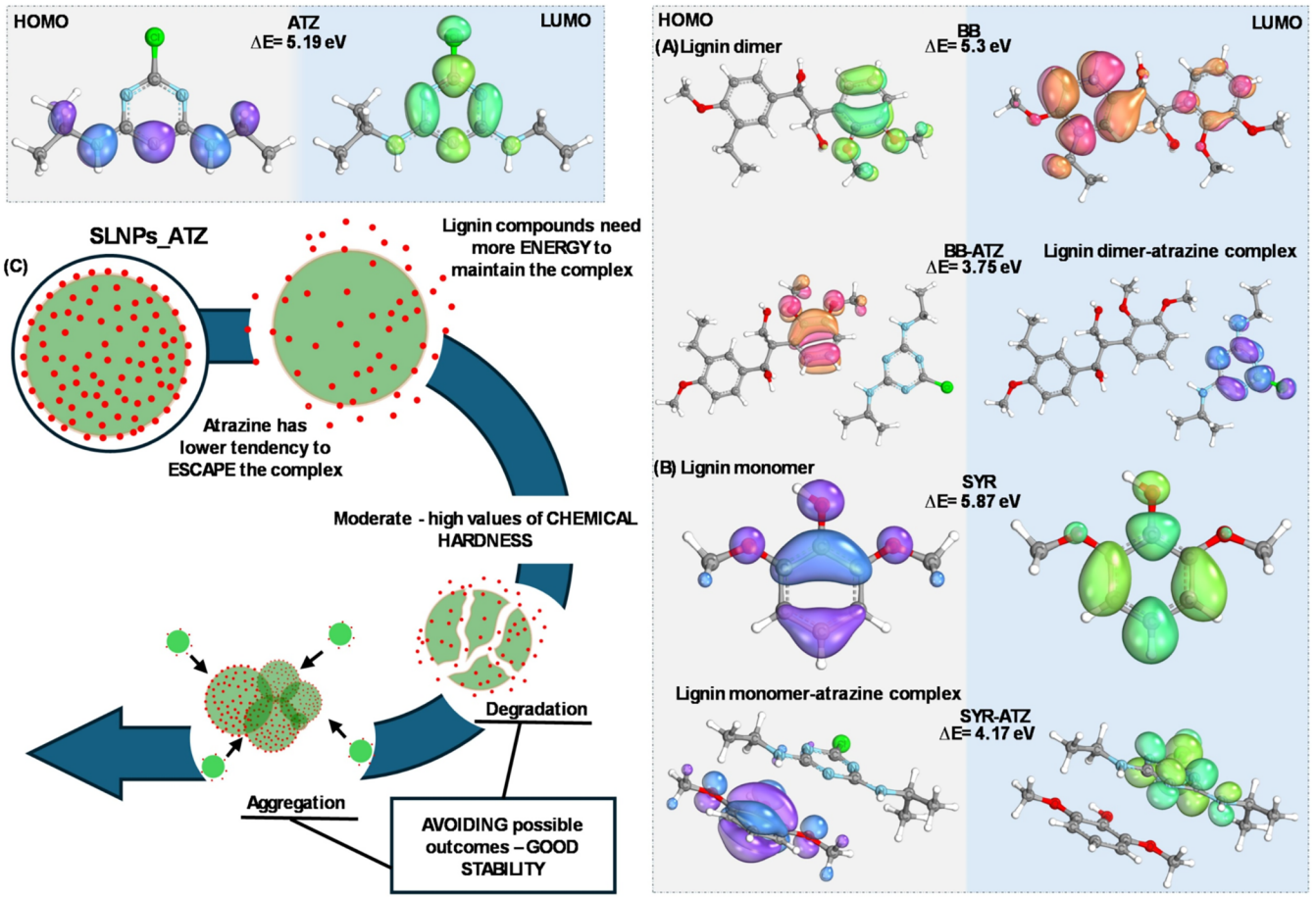

Figure 3. LUMO and HOMO (DFT results) of ATZ: (A) lignin dimer bibenzyl and the interaction of ATZ andbibenzyl, (B) lignin monomer syringol (SYR) and the interaction of ATZ and SYR, and (C) potential scheme of release profile: energy to maintain the complex and stability evaluation of the SLNPs_ATZ.

adsorption), and part was loaded. This behavior, that is, the decrease in T_g values of nanoparticles when loading herbicides, was observed in PLA nanoparticles and metribuzin (MTZ).[65,66]

Subsequently, more formulations were prepared to perform stability tests over time, and nanoparticles without/with atrazine showed sizes (Figure S3A) of 178.96 ± 60.88/268.20 ± 69.58 nm on the first day of analysis by DLS with ζ-potential of −26.43 ± 1.36/−30.83 ± 2.45 mV (Figure S3B) and a polydispersity index (PdI) (Figure S3C) of 0.44 ± 0.16/0.46 ± 0.16. On the last day (seventh), the nanoparticles (with and without atrazine) had sizes of around 151.80 ± 5.79/208.50 ± 7.68 nm, ζ-potential of −31.70 ± 2.76/−22.61 ± 0.94 mV, and a PdI of 0.29 ± 0.08/0.29 ± 0.08. Nanoparticles with ζ-potential above ±30/±20 mV presented good electrostatic/steric stabilization,[67] and the stability of nanoparticles over time is important for storage. Our lignin nanoparticles presented excellent stability after 70 days, which may be caused by the electrostatic repulsion forces on their surface among hydroxyl groups and π−π stacking interactions. The pH stability of nanoparticles is also important since a dispersion that fits the range between 3 and 9 can be considered stable. Our formulations presented a pH of 6.22 for SLNPs and 6.51 for SLNPs_ATZ on the first day and 6.83 and 6.48 on day 70. In fact, the pH values did not vary significantly over time (Figure S3D) and remained around 6−7.[68] Furthermore, the

https://doi.org/10.1021/acssuschemeng.5c05651
ACS Sustainable Chem. Eng. 2025, 13, 15460−15477

loading efficiency was studied, and 74.2% in a 2.75:1 AL/ATZ (w/w) was found, suggesting an interaction between lignin nanoparticles and the active ingredient. For comparison, Dai et al. achieved a loading efficiency of 71.2% while carrying using resveratrol (dissolution of 100 mg/L in water, and 33 mg/L in atrazine) in a proportion of 2:1 AL/resveratrol.[30] Also, Carvalho et al. presented an encapsulation efficiency of above 90% for zein nanoparticles with poloxamer and polysorbate (as surfactants).[69] Moreover, polycaprolactone (PCL) nanocapsules presented an encapsulation efficiency of above 84% for atrazine.[70] It is important to reinforce that most nanocarriers of atrazine have surfactants/oils. On the other hand, our formulation contains only alkali lignin and water, reducing the amount of chemicals and the product's final cost.

The release kinetics profile of herbicide carried by SLNPs_ATZ was determined using a two-compartment assay, as previously described by Grillo et al., where only free ATZ passed through the cellulose membrane. Atrazine release (Figure 2A) reached 43.26% in 168 h.[71] For comparison, Takeshita et al. prepared nanoparticles of polycaprolactone (PCL) carrying MTZ and PCL-lignin-MTZ and compared their release in the first 24 h. PCL-MTZ reached 70% of release, and PCL-lignin-MTZ presented 31.67%, indicating a higher interaction between lignin and the bioactive compound. A similar result was obtained, reaching a 27% release in 24 h and 43.26% after 168 h; this indicates strong lignin−atrazine interactions. The Korsmeyer−Peppas (Figure 2B) model fit the release profile, where the release rate was considerably high in the initial hours and tapered off over time.[12] By the equation in Figure 2B, the slope of the curve is the diffusion index (n) of 0.2553, and n values less than 0.45 follow the Fickian diffusion mechanism.[72] Other kinetic models are provided in Table S3.

3.2. DFT Studies and Chemical Reactivity. Understanding the interactions of organic materials by molecular modeling techniques, such as DFT computational modeling, which allows the identification of essential points on the potential energy surface, has become crucial for exploring and reproducing in the laboratory.[73,74] In this work, DFT studies showed the highest occupied molecular orbital (HOMO) and the lowest unoccupied molecular orbital (LUMO) of atrazine and two model compounds: bibenzyl (BB) and 2-phenethyl phenyl ether (PPE) dimers models of lignin that have already been used in DFT studies.[33] Also, four common monomers were used: syringol (SYR), guaiacol (GUA), vanillyl alcohol (VAL), and vanillic acid (VAN), where SYR has one alcohol and two ethers, GUA has one alcohol and one ether, VAL has two alcohols and one ether, and VAN has an ether, an alcohol, and a carboxylic acid group.[34] This was done to obtain a range of monomers with different functional groups. DFT studies were extremely important to understand the interaction among the molecules because the kinetic stability and chemical reactivity of the systems could be estimated with LUMO and HOMO values, considering that only ATZ, lignin, and water as a solvent were involved.[75]

The LUMO−HOMO gap value of 5.19 eV for ATZ in water (Figure 3) and 5.77 eV for the compound without water matched with the values reported in the literature (5.7−6.0 eV).[76,77] The BB energy gap was around 5.3 eV (Figure 3A), and the complex (BB−ATZ) in water had a lower energy gap of 3.75 eV. Usually, a decrease in the energy gap indicates better stability between the two compounds.[78] The same behavior was observed with the dimer PPE (5.21−4.24 eV) and all monomers: SYR (5.87−4.17 eV) (Figure 3B), GUA (5.57−4.73 eV), VAL (5.37−4.29), and VAN (4.64−4.45) when interacting with ATZ (Figure S4). DFT studies have also complemented experimental investigations by providing insights into nanosystem loading efficiencies and release mechanisms through a theoretical and experimental combination.[79] Therefore, chemical properties (Table 2) were calculated with LUMO and HOMO values, and emerging chemical properties, such as electronic chemical potential (μ), were calculated, which indicates the electrons' tendency to escape from an organic complex, and the direction of electron flow through a molecule's structure. In this work, slightly higher results of all lignin compounds with ATZ compared to ATZ-free were observed, indicating a low ATZ tendency to leave the complex (Figure 3C) and a possible slower release profile. Hence, higher chemical potential values indicate more electrophile complexes.[80]

Table 2. HOMO, LUMO, Chemical Potential (μ), Chemical Hardness (η), Softness (S), and Electrophilicity Index (ω)

structure	E_{HOMO} (eV)	E_{LUMO} (eV)	μ (eV)	η (eV)	S (eV^{-1})	ω (eV)
ATZ	−6.61	−1.42	−4.015	2.595	0.3854	4.03
BB	−5.63	−0.33	−2.980	2.650	0.3774	1.67
PPE	−5.61	−0.40	−3.000	2.600	0.3846	1.73
SYR	−5.82	0.05	−2.885	2.935	0.3407	1.42
GUA	−5.87	−0.30	−3.085	2.785	0.3591	1.71
VAL	−5.74	−0.37	−3.055	2.685	0.3724	1.74
VAN	−6.16	−1.52	−3.840	2.320	0.4310	3.18
BB-ATZ	−5.62	−1.87	−3.745	1.875	0.5333	3.74
PPE-ATZ	−5.60	−1.36	−3.480	2.110	0.4739	2.87
SYR-ATZ	−5.79	−1.62	−3.705	2.085	0.4796	3.29
GUA-ATZ	−5.82	−1.09	−3.455	2.365	0.4228	2.52
VAL-ATZ	−5.68	−1.39	−3.535	2.145	0.4662	2.92
VAN-ATZ	−6.11	−1.66	−3.885	2.225	0.4494	3.39

Moreover, the electrophilicity index (ω) is a property that quantifies the amount of energy required to maintain a stable molecule during electron transportation; a lower ω indicates higher resistance to electron exchange with the environment. Our work found higher values for all complexes when compared to lignin dimers/monomers, which may indicate that more energy (Figure 3C) is necessary to maintain the nanocarrier by lignin compounds.[79] The chemical hardness (η) measures the resistance of a molecule to change the number of electrons in the system; higher values of η indicate a more stable complex, and softness (S) is the capacitance of the molecule to acquire charge.[81,82] Our values of chemical hardness diminish in the order ATZ (2.95 eV), BB (2.65), and PPE (2.6 eV) to ATZ−PPE (2.11) and ATZ−BB (1.875) for dimers; also, all the complexes with monomers had similar behavior. Although a value of around 1.8 eV is moderate to high, indicating that the lignin−atrazine complex is stable after formation, avoiding (Figure 3C) possible rapid degradation or aggregation,[83] the interaction between ATZ and lignin elucidated by DFT correlates with the previously observed: higher loading efficiency and slow-release behavior.[84,85]

3.3. Physiological and Biochemical Assessments. *3.3.1. Physiological Assessments of Exposed Lettuce.* Recently, a work published by Parkinson et al. reported that organic (or soft) nanoparticles with negatively charged surfaces can gradually accumulate in the xylem of roots, putting our

https://doi.org/10.1021/acssuschemeng.5c05651
ACS Sustainable Chem. Eng. 2025, 13, 15460−15477

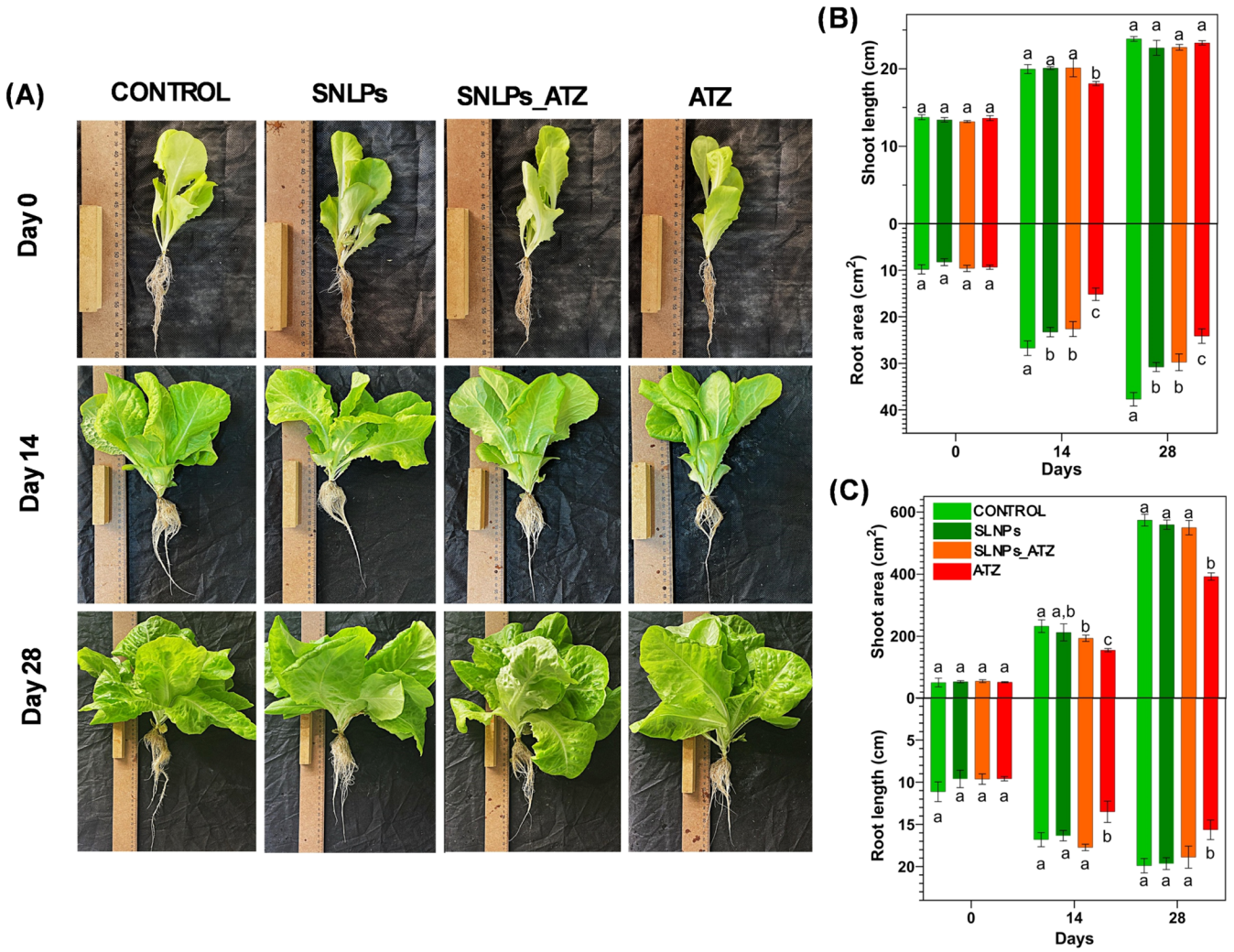

Figure 4. (A) Photos of lettuce with the four treatments at days 0, 14, and 28, (B) lettuce root and shoot lengths, and (C) shoot and root areas. SLNPs and ATZ contained 30 μg/L ATZ. Both formulations (SLNPs_ATZ and ATZ) contained 30 μg/L ATZ. Statistical analysis was performed using two-way ANOVA, and pairwise multiple comparisons and Tukey tests were used to analyze significance (α = 0.05) via GraphPad Prism 8.0.

nanoparticles in a relevant position.[86] Of course, all discussions about nanoherbicides and nontarget species are in their initial phases,[87] and our research focuses on negatively charged organic nanoparticles originating from plants (lignin) to evaluate the hazardous effects in nontarget plants (e.g., lettuce) and aims to enrich future knowledge in modern agro-nanotechnology.

Many herbicides in soil/aquatic systems accumulate in specific organelles/tissues and can face plant detoxification mechanisms when absorbed by roots/shoots, modifying plant morphology. Atrazine herbicide (in lethal doses) can attack nontarget roots of some plants, such as lettuce, and their lengths may serve as important bioindicators of pesticide damage.[88−91] A ruler with a handle was used to compare lettuce (Figure 4A) on days 0, 14, and 28 with all treatments, and the root length (Figure 4B) had significant changes compared to the control, SLNPs, SLNPs_ATZ, and ATZ (day 0: 11.1, 9.6, 9.6, and 9.6 cm, to day 28: 19.9, 19.6, 18.9, and 15.6 cm), presenting a difference of 27.56% between atrazine (30 μg/L) and control, while SLNPs and SLNPs_ATZ presented no significant changes. In another study, treatment with ATZ statistically presented the most drastic difference compared to the control, and lettuce seedlings were reported to have a 33.1% decrease in the root length with 10 μg/L atrazine in 125 h.[92] Moreover, the shoot area (Figure 4C) increased similarly to the root length (% increase in the shoot area compared to days 0 and 28: control, 1027%; SLNPs, 947%; SLNPs_ATZ, 869%; and ATZ, 654%).

Although the root area (Figure 4C) had a significant change between control, SLNPs, SLNPs_ATZ, and ATZ, with SLNPs and SLNPs_ATZ having the same significance (higher than ATZ and lower than control), inferences in root growth by nanoparticles are suggested; however, the increase was comparable to that of ATZ (% increase at day 28: control, 284%; SLNPs, 273%; SLNPs_ATZ, 210%, and ATZ, 159%). Shoot length (Figure 4B) did not show significant changes over time. Nonetheless, the leaf width and area (Figure S5A,B) exhibited changes. For instance, plants exposed to atrazine had 23.43 and 32.76% smaller widths and area sizes than those of the control. Moreover, the results of plants exposed to atrazine compared to SLNPs_ATZ and SLNPs had similar behavior (33−23% area: width smaller than plants with SLNPs_ATZ; 41.15−37.64% area: width smaller than plants with SLNPs). SLNPs did not interfere with the leaf sizes while interacting with nontarget species, such as butterhead lettuce. Curiously, xenobiotic chemicals such as atrazine may cause various

https://doi.org/10.1021/acssuschemeng.5c05651
ACS Sustainable Chem. Eng. 2025, 13, 15460−15477

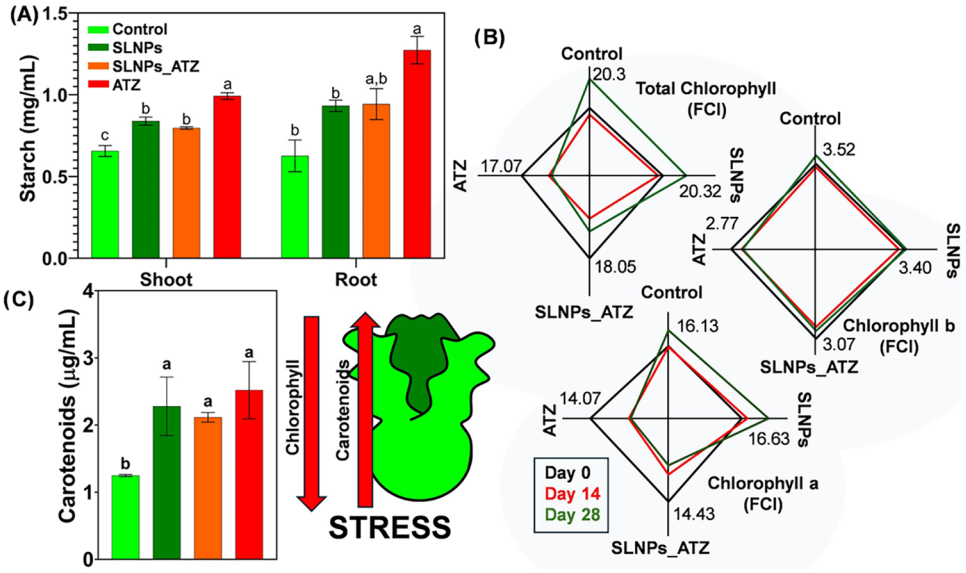

Figure 5. (A) Starch content levels after 28 days, (B) total chlorophyll and chlorophyll *a* and *b* levels at days 0, 14, and 28, and (C) carotenoid levels after 28 days. Both formulations (SLNPs_ATZ and ATZ) contained 30 μg/L ATZ. Statistical analysis was performed by two-way ANOVA, and pairwise multiple comparisons and Tukey tests were used to analyze significance (α = 0.05) via GraphPad Prism 8.0.

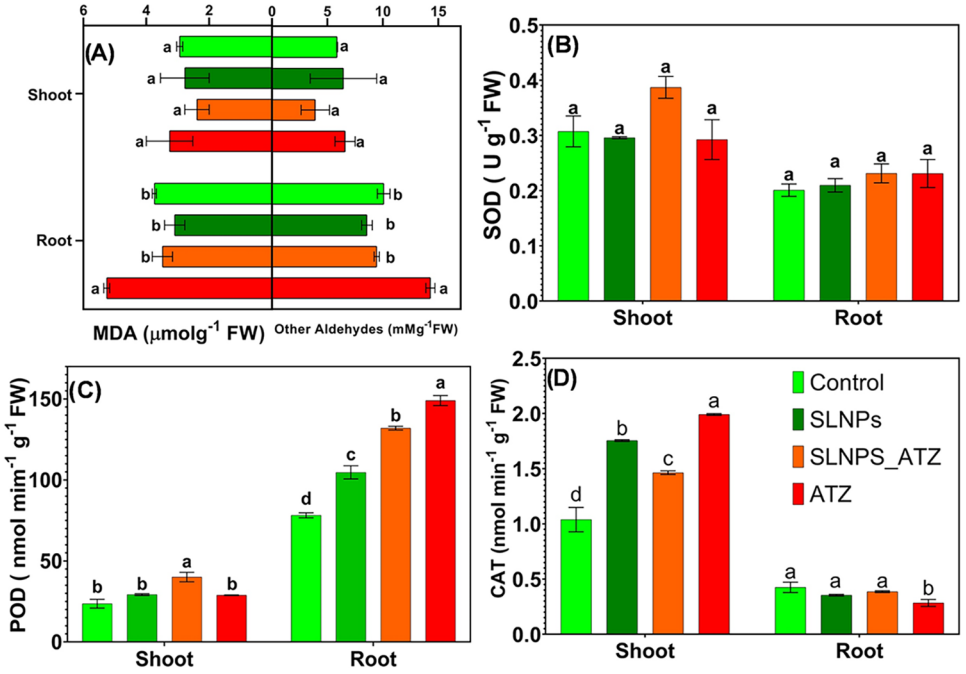

Figure 6. ROS (A) MDA and other aldehydes, (B) SOD, (C) POD, and (D) CAT. Both formulations (SLNPs_ATZ and ATZ) contained 30 μg/L ATZ. Statistical analysis was performed by two-way ANOVA, and pairwise multiple comparisons and Tukey tests were used to analyze significance (α = 0.05) via GraphPad Prism 8.0.

detrimental effects, such as shoot deformation and reduction in the leaf size, but SLNPs_ATZ also did not cause leaf damage.[91]

3.3.2. Starch, Chlorophyll, and Carotenoids. Long-term starch storage provides resources for plants to recover after damage and assists plants in resisting external stresses.[93] After 28 days (Figure 5A), we observed a concentration of 0.656 mg/mL in the control, 0.839 mg/mL in the SLNPs, 0.797 mg/mL in the SLNPs_ATZ, and 0.992 mg/mL in the ATZ in the lettuce shoots, where ATZ presented a statistically significant increase compared to the nanoparticles and control. Additionally, lettuce treated with nanoparticles presented intermediate behavior, with a notably increased value compared to the control. Starch in lettuce root exhibited a slightly different behavior (control, SLNPs, SLNPs_ATZ, ATZ: 0.626, 0.932, 0.943, 1.273 mg/mL, respectively), whereas the control and SLNPs presented a similar behavior. ATZ exhibited a significant increase compared to the control and SLNPs, and SLNPs_ATZ had an intermediate value. These findings are comparable to those of Jiang et al., who reported that atrazine deeply interferes with starch synthesis in soybean leaves (off-target plants), accelerating starch accumulation and enhancing atrazine stress resistance.[94] By FTIR analysis of leaves and roots (Figure S5C,D), which revealed a peak at around 1000

https://doi.org/10.1021/acssuschemeng.5c05651
ACS Sustainable Chem. Eng. 2025, 13, 15460−15477

cm^{-1} associated with carbohydrates, indicating a correlation with starch accumulation, as starch is a carbohydrate. Lettuce exposed to only atrazine showed a significant difference compared to nanoparticles and control.[50]

Atrazine is a known herbicide that inhibits chlorophyll by retarding protoporphyrin IX formation, a chlorophyll synthesis precursor.[95] Atrazine also influences enzymatic mechanisms, such as those involving peroxidase, catalase, and carotenoids.[96] Carotenoids influence photosynthesis and antioxidant activity and contribute to the removal of reactive oxygen species (ROS).[97] After 28 days, our study (Figure 5B) found an increase in total chlorophyll and chlorophyll *a* and *b* (control: 7.82, 4.19, and 9.97%; SLNPs: 6.76, 7.08, and 1.87%) in both untreated plants and those treated with SLNPs, with no statistical difference between the two treatments. On the other hand, plants treated with SLNPs_ATZ and ATZ showed a decrease in all chlorophyll levels (Table S4): SLNPs_ATZ (total chlorophyll: −7.53%; chlorophyll *a*: −9.39%, and chlorophyll *b*: −8.78%) and ATZ (total chlorophyll: −8.81%; chlorophyll *a*: −10.58%, and chlorophyll *b*: −13.45%).

SLNPs_ATZ presented no significant changes in chlorophyll *b* levels compared to SLNPs; however, a considerable difference was observed compared to ATZ. Also, ATZ and SLNPs_ATZ had a significant gap compared to control/SLNPs in total chlorophyll, indicating no chlorophyll synthesis disturbance from SLNPs. The carotenoid concentration in the control (Figure 5C) was 83.06% lower than that in SLNPs, 73.06% lower than that in SLNPs_ATZ, and 102% lower than that in ATZ. Also, the control presented a significant difference compared to all the other treatments. Usually, carotenoids accumulate in plants under abiotic stress (such as atrazine herbicides), and this work obtained comparable results.[98]

3.3.3. Antioxidant Enzymes (ROS). Primary antioxidant enzymes are a class of proteins and metalloproteins that first react with and rapidly catalyze reactive oxygen species into more stable ones. ROS levels increase in response to detrimental pesticidal effects on plants, counteracting their toxicity through metabolic processes in their many internal defense systems to detoxify and/or decompose these chemicals.[91,99,100] MDA is a ROS parameter that measures lipid peroxidation related to the rupture of the cell membranes. MDA levels in lettuce exposed to atrazine (Figure 6A) revealed no significant changes in the shoots. However, the MDA levels in roots showed significant differences when comparing ATZ with all the other treatments (40.51, 69.83, and 50.92% higher than control, SLNPs, and SLNPs_ATZ).[101] For a possible nanoparticle comparison, 0.02 mg/mL of lignin−graft−poly-(lactic-*co*-glycolic) acid (PLGA) nanoparticles (ζ-potential of around −53.6 mV) in a soybean germination hydroponic environment demonstrated no significant MDA changes when compared to control after 14 days, despite our concentration being 667 times (30 μg/L) lower than that of Salinas et al.,[102] and no significant changes were found between SLNPs and control in shoots. It is important to highlight that the monomers of PLGA, lactic acid and glycolic acid, participate in plant life cycles,[103,104] and our concentration was very low because lettuce seedlings died within 8 days in a 300 μg/L ATZ, an undesirable effect over a longer time.

In another work, nanoparticles containing polycaprolactone and lignin carrying the herbicide metribuzin (MTZ) were indicated to have a triple efficiency in killing *Amaranthus retroflexus* compared to PCL−MTZ nanoparticles at 48 g a.i. ha^{-1} after 21 days of application, while PCL−lignin−MTZ showed a less concentrated significant MDA content than PCL−MTZ nanoformulations at 480 g a.i. ha^{-1} in soybean (nontarget) plants.[12] Furthermore, in our research, other aldehydes showed similar results: atrazine had a significant difference compared to other treatments in the root (41.18, 66.76, and 51.14% higher than the control, SLNPs, and SLNPs_ATZ).

Xenobiotic/nonxenobiotic organic nanoparticles have been effectively tested in nontarget plants to understand the limits and effects of their usage. For example, zein/poloxamer nanoparticles were recently reported to be good nanocarriers of glyphosate with no apparent damage in cotton/soy and to show the effects on soil enzymes.[105] On the other hand, chitosan (xenobiotic) nanoparticles (positively charged surfaces) were used as paraquat (a nonselective herbicide) carriers and tested in spinach plants (leaves). Pontes et al. reported a significant change in CAT enzyme level concentration at 20 μg/L when comparing the herbicide to the paraquat-loaded chitosan nanoparticles. Also, chitosan nanoparticles presented significant CAT content changes compared to the paraquat-loaded chitosan nanoparticles at 30 μg/L exposure.[106]

Catalase, a key antioxidant enzyme in aerobic organisms such as plants, belongs to the peroxidase family and catalyzes the breakdown of two hydrogen peroxide molecules (H_2O_2) into water and molecular oxygen in a 2:1 ratio.[100,107] In a work published by Takeshita et al., significant statistical differences among control, MTZ, PCL−MTZ, and PCL−lignin−MTZ in CAT were observed after 30 days in soybean plants exposed to particles.[12] Our work (Figure 6B) presented significant changes in the lettuce treated with ATZ compared to the other treatments, with lower levels of CAT at the root. However, shoot leaves showed significant changes when comparing ATZ to the control (91.71%), SLNPs (68.71%), and SLNPs_ATZ (40.65%), where SLNPs presented more significant levels of POD than SLNPs_ATZ, but lower CAT levels were indicated by SLNPs and SLNPs_ATZ.

SOD is another primary responsive enzyme that removes O_2 radicals from phospholipid membranes.[108] SOD (Figure 6C) showed no significant changes after 28 days in our work, although plants treated with SLNPs_ATZ and ATZ had apparent differences in the shoot area. Moreover, guaiacol peroxidase (POD) is a glycoprotein from the cell wall that is involved in fundamental processes such as defense against abiotic/biotic stress and lignification of cell walls.[109] Guaiacol is commonly used to evaluate peroxidase activity since it oxidizes and turns into tetraguaiacol (which has the maximum absorbance at 470 nm) in the presence of hydrogen peroxide.[110,111] Our research found considerable results when comparing all treatments (Figure 6D). In the shoot (leaves) part, SLNPs_ATZ showed a significantly higher POD concentration. However, SLNPs showed a statistical similarity with the control and SLNPs_ATZ/ATZ. Furthermore, a significant decrease in concentration was observed in the roots (ATZ > SLNPs_ATZ > SLNPs > Control).

3.3.4. Effect of Treatments on Defense Genes (RT-qPCR). Reverse-transcription quantitative polymerase chain reaction (RT-qPCR) was performed to quantify the effects of different treatments (control, SLNPs, SLNPs_ATZ, and ATZ). This study selected GAPDH as a reference gene due to its better stability than that of other genes, such as actin, ubiquitin, and protein phosphatase.[112] For instance, PER51, CAT1, and

https://doi.org/10.1021/acssuschemeng.5c05651
ACS Sustainable Chem. Eng. 2025, 13, 15460−15477

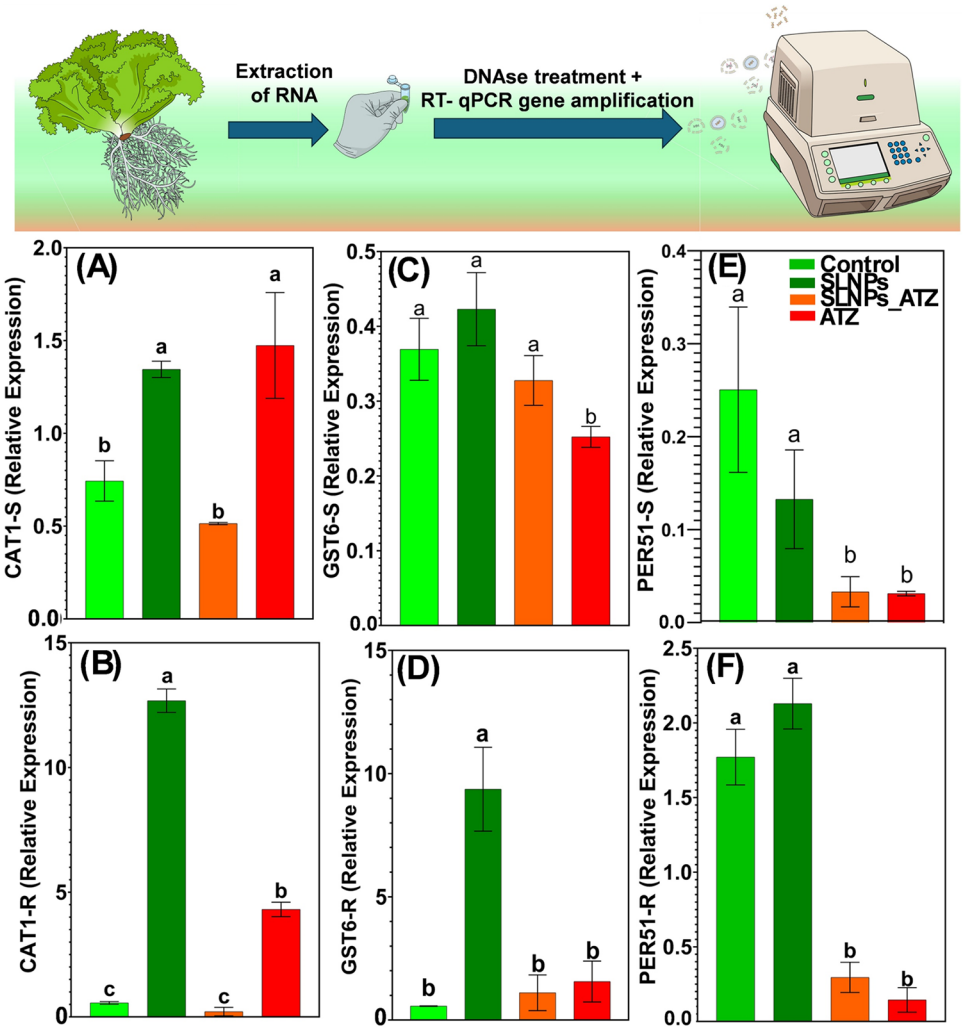

Figure 7. Relative expression of (A, B) CAT1, (C, D) GST6, and (E, F) PER51 genes. Both formulations (SLNPs_ATZ and ATZ) contained 30 μg/L ATZ. Statistical analysis was performed by two-way ANOVA, and pairwise multiple comparisons and Tukey tests were used to analyze significance (α = 0.05) via GraphPad Prism 8.0.

GST6 genes were studied by Chowdhury et al., who used *Arabidopsis thaliana* as the genetic model organism for lettuce and confirmed all the sequences.[47] Also, all these genes (PER51, CAT1, and GST6) have been previously tested for abiotic stress in lettuce.[48]

First, the catalase1 (CAT1) gene, an antioxidant enzyme that is known to possibly scavenge ROS and protect plant cells from oxidative damage, was tested and presented a significant difference between control, SLNPs (increased 2164%) and atrazine (669%) in roots (Figure 7B). Thus, the same behavior was identified in the shoot (Figure 7A): SLNPs, 81.08%; ATZ, 98.65%. Both presented high gene expression values, although lettuce treated with SLNPs and SLNPs_ATZ showed no significant physiological changes in the shoot/root area and length. It is important to mention that plants normally repress growth as an adaptive strategy to maximize survival, and it was observed in lettuce treated with ATZ.[113]

Glutathione *S*-transferases (GSTs) are a class of enzymes that detoxify chemicals and secondary products of oxidative damage. GST6 genes are expressed in response to auxin, SA, and hydrogen peroxide.[48,114] Increased GST expression levels protect organisms against oxidative stress,[115] and a highly increased (1546%) level was observed by SLNPs treatment in roots (Figure 7D) when compared to the control. Tolerance by lettuce is suggested since no significant physiological changes (only in the root area) were noticed. Inherently, SLNPs_ATZ did not exhibit the same behavior, showing no significant changes, representing a possible effect of atrazine that may have downregulated the expression in the root part since GST6 genes in the shoot part (treated with atrazine) presented a significant decrease (46.4%) when compared to the control (Figure 7C).

PER51 genes (Figure 7E,F) participate in Class III peroxidases, which are responsible for functions such as lignification, cell wall biosynthesis, ROS detoxification, and auxin pathway regulation.[116] Recently, PER51 was identified as an LsPRX11 gene by Simoni et al., and they indicated that *LsPRX11 (PER51)* genes are correlated with the regulation of PHR (phosphate starvation response) transcription during P starvation in lettuce.[116,117] Here, they were less resistant in a 30 μg/L atrazine exposure since SLNPs_ATZ and ATZ presented decreasing relative expressions compared to the control in the (SLNPs_ATZ: 86.8%; ATZ: 87.6%) shoots and (SLNPs_ATZ: 83.3%; ATZ: 91.9%) roots, indicating possible repression of these genes caused by atrazine (injuring the plants). Comparable effects were described by Ramel et al.,

https://doi.org/10.1021/acssuschemeng.5c05651
ACS Sustainable Chem. Eng. 2025, 13, 15460−15477

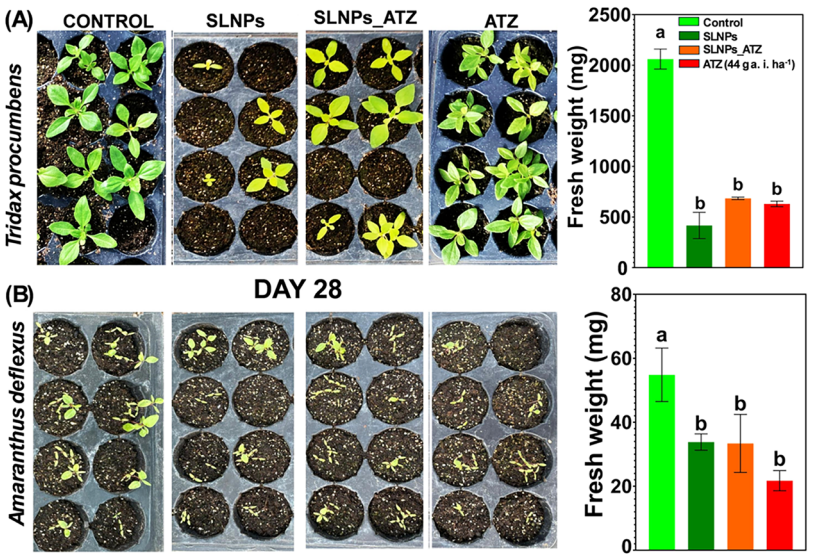

Figure 8. Photos and fresh weights of (A) *T. procumbens* and (B) *A. deflexus* after 28 days. Statistical analysis was performed by two-way ANOVA and pairwise multiple comparisons, and Tukey tests were used to analyze significance (α = 0.05) via GraphPad Prism 8.0.

who observed repression of ascorbate enzyme (a member of the heme-containing peroxidase family) activity and designated a consequent disruption of antioxidant mechanisms by atrazine injuries in *A. thaliana* (a genetic model plant).[118] Moreover, in our research, SLNPs presented a nonsignificant change compared to the control, suggesting that PER51 genes were not affected by the spherical nanoparticles.

It is crucial to highlight that the catalase and peroxidase enzyme activities did not match the gene expression results in our studies. The catalase that was picked, encoded as LOC111878432, has already been used in some recent works with lettuce,[119,120] but is only one of two catalase genes of lettuce (LOC111878431).[121] Then, the possibility that catalase activity is more correlated to the CAT gene LOC111878431 should not be discarded. However, the atrazine levels between enzymatic activity and gene expression in shoots exhibited similar behavior. The same can be inferred from our peroxidase assays; the genes of guaiacol peroxidase (POD) and PER51 genes belong to peroxidase class III, although recently ninety-one peroxidase class III genes were published.[116]

The application of nanoparticles and the upregulation of genes related to biotic and abiotic stress responses are not unusual,[122] and the potential of nanoparticles in enhancing plant tolerance to pollutant stress has been reported in the literature. For example, titanium dioxide nanoparticles were recently identified as a reliever of the atrazine phytotoxicity effect on lettuce.[123] However, the relative expression of genes is not well understood, mainly when the nanoparticles induce expression of specific genes at enormous levels in different treatments. For example, "cold-regulated 413" (COR143) genes play a crucial role in plants stressed by cold and recently showed an upregulation in lettuce treated with carbon dots (nearly ten times higher than the control), where the authors noted a cold tolerance caused by the nanoparticles.[124] For comparison, the values presented here were upregulated around 16 times in the GST6 genes when the control and SLNPs in roots were compared. In another study, biosynthesized silver nanoparticles improved the growth of rice seedlings and had CAT and APX genes upregulated by around 5 and 9 times when comparing rice treated with nanoparticles (10 mg/L) to the control.[125]

The treatment of lettuce with lignin nanoparticles resulted in apparent physiological changes in the root area, which can be related to the plant's mechanism for alleviating stress, which could involve the internalization of SLNPs into vacuoles. However, they did not cause injuries to the plant shoots at the concentrations used (as estimated by NTA data for individual lettuce: ~1.38×10^7 nanoparticles).[4] Moreover, SLNPs_ATZ (as estimated by NTA data for individual lettuce: 278×10^7 nanoparticles) compared to ATZ (30 μg/L) had similar stress behavior in PER51 genes, with SLNPs_ATZ presenting similar physiological changes in lettuce as those treated with SLNPs that reinforce lignin nanoparticles as crop protection at these concentrations. Recently, Javaid et al. produced lignin nanoparticles that effectively promoted sustainable crop production and enhanced abiotic stress tolerance, corroborating the findings of this work.[126] However, studies with higher nanoparticle concentrations are essential to understand the stress versus quantity of nanomaterial behaviors in plants. We theorized that higher SLNP nanoparticle concentrations would result in increased genetic stresses in lettuce and larger physiological changes (phytotoxic effects) in the roots.

Although hydroponics may be excellent inert systems to achieve comparable results, tests in soil (in greenhouses or fields) may have different outcomes. For example, Chang et al. compared wheat and rice exposures to the fungicide phenamacril in hydroponics versus soil conditions and observed overestimated values of translocation factors in hydroponics over soil conditions.[127] For future work, SLNPs in soil conditions with nontarget species would establish new standards for extrapolating the parameters. Moreover, tests using commercial atrazine versus pure atrazine should also be conducted in the future, as previous results showed a less toxic effect from the commercial ATZ than from pure and nanoencapsulated ATZ.[128]

3.4. Preemergent Treatments of Weeds in Sublethal Doses. When 30 μg/L ATZ was used in hydroponic experiments, no lettuce died, since a sublethal dose was applied. Also, the same quantity of bioactive mass was tested

https://doi.org/10.1021/acssuschemeng.5c05651
ACS Sustainable Chem. Eng. 2025, 13, 15460−15477

for soil with ATZ in*T. procumbens* and *A. deflexus* in preemergent treatments in order to observe the different effects between the formulations. Around 270 μg of ATZ was distributed to 16 lettuce plants (16.875 μg per lettuce) in each experiment. Therefore, we treated each pot with the same amount (44 g a.i. ha^{-1}) as explained in the methodology section. Atrazine is typically recommended in doses of around 850 g a.i. ha^{-1} of atrazine (mixed with 1.65 kg i.a. ha^{-1} of metolachlor) for *T. procumbens*.[129] Our research had n = 8 (where n is the number of pots), and pots with control and atrazine treatments had clearly higher germination rates in seeds (Figure 8) than those treated with SLNPs and SLNPs_ATZ.

Seeds treated with ATZ germinated 2.22, 5, and 3.33 times more than the control, SLNPs, and SLNPs_ATZ. Therefore, the effect of hormesis, a phenomenon in which low doses stimulate plant growth and high doses induce inhibition, may be suggested.[130] Although the germination rates were very low in all cases (on day 4: 3.75%, control; 1.25%, SLNPs; 2.5%, SLNPs_ATZ; and 15%, ATZ and on day 8: 11.25%, control; 5%, SLNPs; 7.5%, SLNPs_ATZ; and 25%, ATZ) suggesting hormesis. The germination rate may be due to the number of seeds in a small space (10 seeds at around 38.48 cm^2 of soil) that may have led to competition among seeds over time (Figure S6),[131] or to the strong allelopathy of *T. procumbens*.[132] However, the plants that did germinate had a 100% survival rate for all the treatments, with a notorious fourth time larger growth in fresh weight (Figure 8A) of control (2 g after 28 days) over the others (around 0.5 g).

In contrast, the germination rate in *A. deflexus* seeds preemergence treated was much higher: reaching almost 50% at the control (Figure S7) after 21 days. Moreover, seeds treated with ATZ (44 g a.i. ha^{-1}) had a significant decrease in the germination rate when compared to the control, and similar effects were observed in *A. retroflexus* germination when exposed to several sublethal doses of atrazine (18.75−600 g a.i. ha^{-1}), showing important results such as lower germination percentage between 1/32 (37.5 g a.i. ha^{-1}) and 1/16 (75 g a.i. ha^{-1}) of the recommended dose (1200 g a.i. ha^{-1}) in China.[133] The same behavior was observed in the seeds treated with SLNPs; they presented a decreased germination rate when compared to the control. SLNPs also seem to have a greater effect than SLNPs_ATZ on germination, which could be due to the lower quantity of atrazine in the initial contact between the seed surface and the atrazine-absorbed part (by SLNPs in SLNPs_ATZ). This means that the other quantity (the partially engulfed atrazine) is slowly released (43.26%) later. Therefore, SLNPs_ATZ formulations would provide initial direct contact (with the adsorbed atrazine) and later contact with the released atrazine.[134] SLNPs also genetically expressed higher values of the CAT1 and GST6 genes in lettuce. On the other hand, SLNPs_ATZ showed a germination rate similar to that of the control; however, the weeds presented slower development and final fresh weight (Figure 8B).

In general, nanoparticles with herbicidal effects are seen in the literature as positive signs to lower herbicide doses, and nonxenobiotic and xenobiotic nanoparticles (to plants) have already been related to having higher efficiency in lower doses when compared to atrazine. For example, PCL (xenobiotic) nanocapsules with atrazine presented the same inhibitory effects on root and shoot growth of *Amaranthus viridis* and *Bidens pilosa* seedlings with concentrations ten times lower than conventional (2000 g a.i. ha^{-1}) in Brazil.[135] Moreover, zein (nonxenobiotic) nanoparticles with atrazine had greater herbicidal activity against *Brassica juncea* at doses 80 times (25 g a.i. ha^{-1}) lower than the recommended dose for preemergent treatments.[69] Lignin is a nonxenobiotic material to plants that had already been tested as nanoformulations for other weeds, such as *A. retroflexus* with PCL in preemergent treatments by Takeshita et al., where they observed a fresh mass 3.45 times lower in plants treated with PCL−lignin−MTZ than PCL−MTZ in 48 g a.i. ha^{-1}. They also highlighted the importance of lignin as a natural molecule suitable for safe-by-design herbicide nanoformulations.[12] Moreover, Munhoz et al. presented zein−lignin nanocarriers synthesized with glyphosate as the active ingredient and indicated a reduction or interference of the nanoherbicides in weed plants (*Amaranthus hybridus*, *Ipomoea grandifolia*, and *Eleusine indica*).[136]

Also, lignin has been reported as a matrix for the herbicides pelargonic acid and citronella oil in nanoemulsion formulations to kill *Pennisetum purpureum* (Elephant grass).[137,138] Here, *T. procumbens* (coat buttons) presented lower chlorophyll levels in seedlings (Figure S6) caused by SLNPs and SLNPs_ATZ, apparently developing a malfunction in germination/growth in the presence of spherical lignin nanoparticles after 28 days. Of course, these results may be better evaluated in the future by approaching new concentration variables, time, and post-emergence treatments. However, it is important to highlight the apparent changes caused by lignin nanoparticles and the value of future experiments using lignocellulose materials as the main nanoparticle matrices.

4. CONCLUSIONS

Spherical lignin nanoparticle was fabricated, and the herbicide atrazine was associated by two possible routes: encapsulation and adsorption. Release and DFT experiments were conducted, and strong interactions between lignin and atrazine were observed. Hydroponic experiments showed that butterhead lettuce exhibited physiological changes at a sublethal dose of atrazine (30 μg/L). Lettuce treated with SLNPs and SLNPs_ATZ showed no significant changes in the root length and shoot area compared to the control, while lettuce treated with ATZ did. Biochemical tests, such as enzymatic and relative gene expression, were assessed and showed up- and downregulated behaviors. Finally, weed seeds/seedlings showed possible interference in germination and development caused by nanoherbicides, indicating that lignin is a sustainable molecule capable of forming nanoparticles that can load atrazine and can be effectively used in future experiments with nontarget/target plants, potentially affecting gene expression and weed control outcomes. Also, lignin can be formulated using multiple methods (encapsulation, modification, or in a mixture with other molecules) to enhance its properties and provide sustainability to new nanocarriers in agriculture. In future studies, different concentrations of different types of lignin nanoparticles should be explored.

■ ASSOCIATED CONTENT

Supporting Information

The Supporting Information is available free of charge at https://pubs.acs.org/doi/10.1021/acssuschemeng.5c05651.

Experimental details (Text S1); compounds in fertilizers for the hydroponic tests (Tables S1 and S2); kinetic models (Table S3); chlorophyll levels (Table S4); nanoparticle characterization (Figures S1 and S2);

https://doi.org/10.1021/acssuschemeng.5c05651
ACS Sustainable Chem. Eng. 2025, 13, 15460−15477

nanoparticle analysis over time (Figure S3); DFT interactions (Figure S4); analysis of lettuce (Figure S5); and weed analysis (Figures S6 and S7) (PDF)

AUTHOR INFORMATION

Corresponding Author

Renato Grillo − *São Paulo State University (UNESP), Department of Physics and Chemistry, School of Engineering, Ilha Solteira, SP 15385-007, Brazil;* orcid.org/0000-0002-0284-5782; Phone: +55 18 37431074; Email: renato.grillo@unesp.br

Authors

Pedro H. C. de Lima − *São Paulo State University (UNESP), Department of Physics and Chemistry, School of Engineering, Ilha Solteira, SP 15385-007, Brazil*

Maria C. Shiroma Buri − *São Paulo State University (UNESP), Department of Plant Protection, Rural Engineering and Soils, Ilha Solteira 15385-007, Brazil;* orcid.org/0009-0008-6200-7001

Rafaela S. Mendonça − *São Paulo State University (UNESP), Department of Physics and Chemistry, School of Engineering, Ilha Solteira, SP 15385-007, Brazil*

Gabriel M. Favara − *São Paulo State University (UNESP), Department of Plant Protection, Rural Engineering and Soils, Ilha Solteira 15385-007, Brazil*

Érica R. Biscalchim − *São Paulo State University (UNESP), Department of Physics and Chemistry, School of Engineering, Ilha Solteira, SP 15385-007, Brazil;* orcid.org/0000-0001-9464-5835

Mariana M. L. H. Forini − *São Paulo State University (UNESP), Department of Physics and Chemistry, School of Engineering, Ilha Solteira, SP 15385-007, Brazil*

Luiz A. F. Cavalcante − *São Paulo State University (UNESP), Department of Physics and Chemistry, School of Engineering, Ilha Solteira, SP 15385-007, Brazil*

Complete contact information is available at: https://pubs.acs.org/10.1021/acssuschemeng.5c05651

Author Contributions

P.H.C.d.L., M.C.S.B., R.S.M., and G.M.F.: research, writing, review, and editing the manuscript. E.R.B., M.M.L.H.F., and L.A.F.C.: research and review. R.G.: conceptualization, writing, review, editing, and supervision of the manuscript. All authors have equally contributed to revising and reading the manuscript and have approved the submitted version.

Funding

The Article Processing Charge for the publication of this research was funded by the Coordenacao de Aperfeicoamento de Pessoal de Nivel Superior (CAPES), Brazil (ROR identifier: 00x0ma614).

Notes

The authors declare no competing financial interest.

ACKNOWLEDGMENTS

The authors thank the São Paulo Research Foundation, FAPESP (grants #2021/03402-9, #2022/03219-2, #2023/00541-3, #2023/17369-9), National Council for Scientific and Technological Development, CNPq (grant # 310846/2022-6), and the Coordination of Improvement of Higher Education Personnel (CAPES, Finance Code 001). We also acknowledge the Emergency Support for Multi-User Equipment from the São Paulo State University Vice-Presidency of Research (PROPe), which supported the technical assistance from M.C.S.B. and the Ilha Solteira Microscopy Laboratory, LaMIS.

REFERENCES

(1) Debaeke, P.; Perronne, R.; Colbach, N.; Moreau, D.; Barre, P.; Lecouviour, F.; Durand-Tardif, M. Non-chemical weed management: Which crop functions and traits to improve through breeding? *Crop Prot.* **2024**, *179*, No. 106631.

(2) Perotti, V. E.; Larran, A. S.; Palmieri, V. E.; Martinatto, A. K.; Permingeat, H. R. Herbicide Resistant Weeds: A Call to Integrate Conventional Agricultural Practices, Molecular Biology Knowledge and New Technologies. *Plant Sci.* **2020**, *290*, No. 110255.

(3) Yu, M.; Dong, H.; Liu, K.; Zheng, Y.; Hoffmann, M. R.; Liu, W. Porous carbon monoliths for electrochemical removal of aqueous herbicides by "one-stop" catalysis of oxygen reduction and H2O2 activation. *J. Hazard. Mater.* **2021**, *414*, No. 125592.

(4) Forini, M. M.; Pontes, M. S.; Antunes, D. R.; de Lima, P. H.; Santos, J. S.; Santiago, E. F.; Grillo, R. Nano-enabled weed management in agriculture: From strategic design to enhanced herbicidal activity. *Plant Nano Biol.* **2022**, *1*, No. 100008.

(5) Cheng, J.; Li, M.; Zhu, R. X.; Li, J. Y.; Yin, J.; Xiao, W. A timing self-cleaning nanoherbicide: Design of triple-structure nanovectors for weed control and pesticide residues treatment. *Adv. Agrochem* **2024**, *3* (4), 298−307.

(6) Kusumavathi, K.; Rautaray, S. K.; Sarkar, S.; Dash, S.; Sahoo, T. R.; Swain, S. K.; Sethi, D. Nano-herbicides a sustainable strategy for weed control. *Plant Nano Biol.* **2025**, *11*, No. 100132.

(7) Österberg, M.; Sipponen, M. H.; Mattos, B. D.; Rojas, O. J. Spherical Lignin Particles: A Review on Their Sustainability and Applications. *Green Chem.* **2020**, *22* (9), 2712−2733.

(8) Anushikha; Gaikwad, K. K. Lignin as a UV blocking, antioxidant, and antimicrobial agent for food packaging applications. *Biomass Convers. Biorefin.* **2024**, *14* (15), 16755−16767.

(9) Trevisan, H.; Rezende, C. A. Pure, stable and highly antioxidant lignin nanoparticles from elephant grass. *Ind. Crops Prod.* **2020**, *145*, No. 112105.

(10) de Lima, P. H. C.; Antunes, D. R.; Forini, M. M. D. L.; Pontes, M. D. S.; Mattos, B. D.; Grillo, R. Recent advances on lignocellulosic-based nanopesticides for agricultural applications. *Front. Nanotechnol.* **2021**, *3*, No. 809329.

(11) Ma, Y.; Remón, J.; Luo, L.; Ding, W.; Jiang, Z.; Shi, B. Natural-Based UV-Shielding Additives to Protect Photosensitive Pesticides: Production of Nanoparticles from the Co-Self-Assembly of Lignin and Tannin. *Nano Today* **2025**, *60*, No. 102550.

(12) Takeshita, V.; Oliveira, F. F.; Garcia, A.; Zuverza-Mena, N.; Tamez, C.; Cardoso, B. C.; White, J. C.; et al. Delivering metribuzin from biodegradable nanocarriers: assessing herbicidal effects for soybean plant protection and weed control. *Environ. Sci.: Nano* **2025**, *12*, 388−404, DOI: 10.1039/D4EN00784K.

(13) Gajendra, G.; Pulimi, M.; Natarajan, C.; Mukherjee, A. Occurrence, Toxicodynamics, and Mechanistic Insights for Atrazine Degradation in the Environment. *Water, Air, Soil Pollut.* **2024**, *235* (10), 649.

(14) Jiang, Z.; Shao, Q.; Chu, Y.; An, N.; Cao, B.; Ren, Z.; Zhang, Y.; et al. Mitigation of atrazine-induced oxidative stress on soybean seedlings after co-inoculation with atrazine-degrading bacterium Arthrobacter sp. DNS10 and inorganic phosphorus-solubilizing bacterium Enterobacter sp. P1. *Environ. Sci. Pollut. Res.* **2023**, *30* (11), 30048−30061.

(15) Wu, J.; Zhai, Y.; Monikh, F. A.; Arenas-Lago, D.; Grillo, R.; Vijver, M. G.; Peijnenburg, W. J. The differences between the effects of a nanoformulation and a conventional form of atrazine to lettuce: physiological responses, defense mechanisms, and nutrient displacement. *J. Agric. Food Chem.* **2021**, *69* (42), 12527−12540.

(16) Zhai, Y.; Monikh, F. A.; Wu, J.; Grillo, R.; Arenas-Lago, D.; Darbha, G. K.; Vijver, M. G.; Peijnenburg, W. J. G. M. Interaction

between a nano-formulation of atrazine and rhizosphere bacterial communities: atrazine degradation and bacterial community alterations. *Environ. Sci.: Nano* **2020**, *7*, 3372−3384.
(17) Akpinar, I.; Drout, R. J.; Islamoglu, T.; Kato, S.; Lyu, J.; Farha, O. K. Exploiting $\pi-\pi$ interactions to design an efficient sorbent for atrazine removal from water. *ACS Appl. Mater. Interfaces* **2019**, *11* (6), 6097−6103.
(18) Wang, N.; Cheng, X.; Li, N.; Wang, H.; Chen, H. Nanocarriers and their loading strategies. *Adv. Healthcare Mater.* **2019**, *8* (6), No. 1801002.
(19) Grillo, R.; Mattos, B. D.; Antunes, D. R.; Forini, M. M. L.; Monikh, F. A.; Rojas, O. J. Foliage Adhesion and Interactions with Particulate Delivery Systems for Plant Nanobionics and Intelligent Agriculture. *Nano Today* **2021**, *37*, No. 101078.
(20) Grillo, R.; Fraceto, L. F.; Amorim, M. J. B.; Scott-Fordsmand, J. J.; Schoonjans, R.; Chaudhry, Q. Ecotoxicological and Regulatory Aspects of Environmental Sustainability of Nanopesticides. *J. Hazard. Mater.* **2021**, *404*, No. 124148.
(21) Lei, C.; Engeseth, N. J. Comparison of growth characteristics, functional qualities, and texture of hydroponically grown and soil-grown lettuce. *LWT* **2021**, *150*, No. 111931.
(22) Chowdhury, M.; Samarakoon, U. C.; Altland, J. E. Evaluation of hydroponic systems for organic lettuce production in controlled environment. *Front. Plant Sci.* **2024**, *15*, No. 1401089.
(23) Li, Y.; Lin, X.; Xu, G.; Yan, Q.; Yu, Y. Toxic effects and mechanisms of engineered nanoparticles and nanoplastics on lettuce (*Lactuca sativa* L.). *Sci. Total Environ.* **2024**, *908*, No. 168421.
(24) Yao, T.; Feng, K.; Xie, M.; Barros, J.; Tschaplinski, T. J.; Tuskan, G. A.; Muchero, W.; Chen, J. G. Phylogenetic occurrence of the phenylpropanoid pathway and lignin biosynthesis in plants. *Front. Plant Sci.* **2021**, *12*, No. 704697.
(25) Xie, J.; Cao, B.; Xu, K. Uncovering the dominant role of root lignin accumulation in silicon-induced resistance to drought in tomato. *Int. J. Biol. Macromol.* **2024**, *259*, No. 129075.
(26) de Souza, V. V.; da Silva Souza, T.; de Campos, J. M. S.; de Oliveira, L. A.; Ribeiro, Y. M.; de Melo Hoyos, D. C.; Lacerda, S. M. D. S. N.; et al. Ecogenotoxicity of environmentally relevant atrazine concentrations: a threat to aquatic bioindicators. *Pestic. Biochem. Physiol.* **2023**, *189*, No. 105297.
(27) Pérez, D. J.; Doucette, W. J.; Moore, M. T. Atrazine Uptake, Translocation, Bioaccumulation and Biodegradation in Cattail (*Typha latifolia*) as a Function of Exposure Time. *Chemosphere* **2022**, *287*, No. 132104.
(28) Preisler, A. C.; Carvalho, L. B.; Saraiva-Santos, T.; Verri, W. A., Jr.; Mayer, J. L. S.; Fraceto, L. F.; Dalazen, G.; Oliveira, H. C. Interaction of Nanoatrazine and Target Organism: Evaluation of Fate and Photosystem II Inhibition in Hydroponically Grown Mustard (*Brassica juncea*) Plants. *J. Agric. Food Chem.* **2022**, *70* (25), 7644−7652.
(29) Sousa, B. T.; Carvalho, L. B.; Preisler, A. C.; Saraiva-Santos, T.; Oliveira, J. L.; Verri, W. A., Jr.; Oliveira, H.; et al. Chitosan Coating as a Strategy to Increase Postemergent Herbicidal Efficiency and Alter the Interaction of Nanoatrazine with *Bidens pilosa* Plants. *ACS Appl. Mater. Interfaces* **2025**, *17* (9), 13122−13134.
(30) Dai, L.; Liu, R.; Hu, L. Q.; Zou, Z. F.; Si, C. L. Lignin nanoparticle as a novel green carrier for the efficient delivery of resveratrol. *ACS Sustainable Chem. Eng.* **2017**, *5* (9), 8241−8249.
(31) López-Cabeza, R.; Kah, M.; Grillo, R.; Bílková, Z.; Hofman, J. Is Centrifugal Ultrafiltration a Robust Method for Determining Encapsulation Efficiency of Pesticide Nanoformulations? *Nanoscale* **2021**, *13*, 5410−5418.
(32) Ritger, P. L.; Peppas, N. A. A Simple Equation for Description of Solute Release I. Fickian and Non-Fickian Release from Non-Swellable Devices in the Form of Slabs, Spheres, Cylinders or Discs. *J. Controlled Release* **1987**, *5* (1), 23−36.
(33) Yamaguchi, A.; Mimura, N.; Shirai, M.; Sato, O. Bond cleavage of lignin model compounds into aromatic monomers using supported metal catalysts in supercritical water. *Sci. Rep.* **2017**, *7* (1), No. 46172.
(34) Lu, T.; Wang, J.; Wei, G.; Li, G.; Wang, Y.; Wu, W.; Liang, Y. A combined experimental and theoretical study on vanadium-catalytic oxidation of lignin to produce carboxylic acids. *Fuel Process. Technol.* **2022**, *238*, No. 107493.
(35) Belakhdar, A.; Ferkous, H.; Djellali, S.; Sahraoui, R.; Lahbib, H.; Amor, Y. B.; Benguerba, Y.; et al. Computational and experimental studies on the efficiency of Rosmarinus officinalis polyphenols as green corrosion inhibitors for XC48 steel in acidic medium. *Colloids Surf., A* **2020**, *606*, No. 125458.
(36) Ng, S. W.; Rosli, N. S. M.; Razali, R. B. R.; Abdullah, R.; Yaacob, J. S. From Waste to Wealth: Significant Potential of Oil Palm Kernel-Derived Biochar as Alternative Substrate for Production of Red Lettuce (*Lactuca sativa* L.) with High Bioactive Metabolites Content in NFT Hydroponic System. *Sustainable Chem. Pharm.* **2023**, *34*, No. 101167.
(37) Rawashdeh, R. Y.; Harb, A. M.; AlHasan, A. M. Biological Interaction Levels of Zinc Oxide Nanoparticles; Lettuce Seeds as Case Study. *Heliyon* **2020**, *6* (5), No. e03983.
(38) Antunes, D. R.; Forini, M. M.; Coqueiro, Y. A.; Pontes, M. S.; Lima, P. H.; Cavalcante, L. A.; Grillo, R.; et al. Effect of hyaluronic acid-stabilized silver nanoparticles on lettuce (*Lactuca sativa* L.) seed germination. *Chemosphere* **2024**, *364*, No. 143080.
(39) Wang, J.; Ma, Y.; Huang, X.; Song, L.; Li, N.; Cheng, Y.; Hai, D.; et al. Changes in physio-biochemical metabolism, phenolics and antioxidant capacity of different Chinese pea varieties during germination. *Int. J. Food Sci. Technol.* **2023**, *58* (1), 167−180.
(40) Behtash, F.; Amini, T.; Mousavi, S. B.; Seyed Hajizadeh, H.; Kaya, O. Efficiency of zinc in alleviating cadmium toxicity in hydroponically grown lettuce (*Lactuca sativa* L. cv. Ferdos). *BMC Plant Biol.* **2024**, *24* (1), No. 648.
(41) Fotovvat, M.; Najafi, F.; Khavari-Nejad, R. A.; Talei, D.; Rejali, F. Investigating the simultaneous effect of chitosan and arbuscular mycorrhizal fungi on growth, phenolic compounds, PAL enzyme activity and lipid peroxidation in *Salvia nemorosa* L. *Plant Physiol. Biochem.* **2024**, *210*, No. 108617.
(42) Azevedo, R. A.; Alas, R. M.; Smith, R. J.; Lea, P. J. Response of antioxidant enzymes to transfer from elevated carbon dioxide to air and ozone fumigation, in the leaves and roots of wild-type and a catalase-deficient mutant of barley. *Physiol. Plant.* **1998**, *104* (2), 280−292.
(43) Chance, B.; Maehly, A. C. Assay of Catalases and Peroxidases. In *Methods in Enzymology*, 1955; Vol. 2, pp 764−775.
(44) da Silva Santos, J.; da Silva Pontes, M.; Grillo, R.; Fiorucci, A. R.; de Arruda, G. J.; Santiago, E. F. Physiological mechanisms and phytoremediation potential of the macrophyte Salvinia biloba towards a commercial formulation and an analytical standard of glyphosate. *Chemosphere* **2020**, *259*, No. 127417.
(45) Doyle, J. J.; Doyle, J. L. A rapid DNA isolation procedure for small quantities of fresh leaf tissue. *Phytochem. Bull.* **1987**, *19*, 11−15.
(46) Chowdhury, S. P.; Uhl, J.; Grosch, R.; Alquéres, S.; Pittroff, S.; Dietel, K.; Hartmann, A.; et al. Cyclic lipopeptides of *Bacillus amyloliquefaciens* subsp. plantarum colonizing the lettuce rhizosphere enhance plant defense responses toward the bottom rot pathogen Rhizoctonia solani. *Mol. Plant-Microbe Interact.* **2015**, *28* (9), 984−995.
(47) Paul Chowdhury, S.; Babin, D.; Sandmann, M.; Jacquiod, S.; Sommermann, L.; Sørensen, S. J.; Grosch, R.; et al. Effect of long-term organic and mineral fertilization strategies on rhizosphere microbiota assemblage and performance of lettuce. *Environ. Microbiol.* **2019**, *21* (7), 2426−2439.
(48) Bigott, Y.; Chowdhury, S. P.; Pérez, S.; Montemurro, N.; Manasfi, R.; Schröder, P. Effect of the pharmaceuticals diclofenac and lamotrigine on stress responses and stress gene expression in lettuce (*Lactuca sativa*) at environmentally relevant concentrations. *J. Hazard. Mater.* **2021**, *403*, No. 123881.
(49) Livak, K. J.; Schmittgen, T. D. Analysis of relative gene expression data using real-time quantitative PCR and the $2^{-\Delta\Delta CT}$ method. *Methods* **2001**, *25* (4), 402−408.

(50) Wang, Q.; Wang, H.; Chen, H.; Meng, Z.; Kong, F.; Liu, Y.; Jiang, W. Efficient synthesis of highly hydrophobic lignin nanoparticles and their application as nano fillers for multifunctional composite membranes. *Int. J. Biol. Macromol.* **2024**, *282*, No. 136869.
(51) Wang, H.; Liu, M.; Tan, S.; Li, X.; Huang, M.; Hao, X.; Peng, F. Porous lignin nanospheres as microscopic air purifiers for antioxidant-configurable cigarette filters. *Adv. Funct. Mater.* **2025**, *35*, No. 2420731.
(52) Xing, R.; He, J.; Hao, P.; Zhou, W. Graphene oxide-supported nanoscale zero-valent iron composites for the removal of atrazine from aqueous solution. *Colloids Surf., A* **2020**, *589*, No. 124466.
(53) Wang, Y.; Chen, Y.; Wang, L.; Mo, Y.; Lin, X.; Gao, S.; Chen, M. Efficient removal of atrazine in wastewater by washed peanut shells biochar: Adsorption behavior and biodegradation. *Process Biochem.* **2025**, *154*, 22−34, DOI: 10.1016/j.procbio.2025.04.008.
(54) Lee, J. H.; Kim, K.; Jin, X.; Kim, T. M.; Choi, I. G.; Choi, J. W. Formation of pure nanoparticles with solvent-fractionated lignin polymers and evaluation of their biocompatibility. *Int. J. Biol. Macromol.* **2021**, *183*, 660−667.
(55) Lu, X.; Zhang, Y.; Chen, J.; Zhang, D.; Dong, C.; Zhiqiang, P.; Xia, T. Preparation of tailored lignin nanospheres with specific size and tunable structure by self-assembly of lignin from corn straw. *Ind. Crops Prod.* **2021**, *172*, No. 113993.
(56) Peng, Q.; Ye, L.; Wen, N.; Chen, H.; Zhu, Y.; Niu, H.; Huang, Y.; et al. Nitrogen Vacancy-Modified g-C3N4 Nanosheets Controlled by Deep Eutectic Solvents for Highly Efficient Photocatalytic Atrazine Degradation: Non-Radical Dominated Holes Oxidation. *Sep. Purif. Technol.* **2025**, *354*, No. 128879.
(57) Zhang, Z.; Marin, C. B.; Lefebvre, M.; Lefebvre, C.; Terrasson, V.; Guénin, E. The preparation of stable spherical alkali lignin nanoparticles with great thermal stability and no cytotoxicity. *Int. J. Biol. Macromol.* **2022**, *222*, 1830−1839.
(58) Freitas, F. M.; Cerqueira, M. A.; Gonçalves, C.; Azinheiro, S.; Garrido-Maestu, A.; Vicente, A. A.; Michelin, M.; et al. Green synthesis of lignin nano- and micro-particles: Physicochemical characterization, bioactive properties and cytotoxicity assessment. *Int. J. Biol. Macromol.* **2020**, *163*, 1798−1809.
(59) Xiong, F.; Han, Y.; Wang, S.; Li, G.; Qin, T.; Chen, Y.; Chu, F. Preparation and formation mechanism of size-controlled lignin nanospheres by self-assembly. *Ind. Crops Prod.* **2017**, *100*, 146−152.
(60) Liu, Y.; Jia, L.; Xiao, Y.; Wang, H.; Luo, X.; Wang, S.; Zhou, L.; Yin, Q. Solubility Measurement and Thermodynamic Properties of Atrazine in 13 Pure Solvents from 283.15 to 323.15 K. *J. Chem. Eng. Data* **2025**, *70* (1), 607−618.
(61) Guo, Y.; Xu, L.; Shen, F.; Hu, J.; Huang, M.; He, J.; Tian, D.; et al. Insights into lignocellulosic waste fractionation for lignin nanospheres fabrication using acidic/alkaline deep eutectic solvents. *Chemosphere* **2022**, *286*, No. 131798.
(62) Gong, Y.; Li, S.; Hu, Y.; Jin, G.; Zhou, H.; Lim, L. T.; Xiao, Q. Acidic and alkaline deep eutectic solvents pretreatment of Macadamia nutshells for production of cellulose nanofibrils and lignin nanoparticles. *Int. J. Biol. Macromol.* **2025**, *300*, No. 140251.
(63) Sharma, S.; Kachhia, P.; Shukla, V.; Patel, A.; Rathod, V.; Narra, M. Valorization of lignin into nanoparticles and nanogel: Characterization and application. *Bioresour. Technol. Rep.* **2022**, *18*, No. 101041.
(64) Gautam, T. R.; Vasmatkar, P.; Gundloori, R. V.; Kadoo, N. Ethyl cellulose-based controlled-release atrazine nanoformulation for effective and long-term weed management in agriculture. *Ind. Crops Prod.* **2025**, *229*, No. 120992.
(65) Stloukal, P.; Kucharczyk, P.; Sedlarik, V.; Bazant, P.; Koutny, M. Low molecular weight poly(lactic acid) microparticles for controlled release of the herbicide metazachlor: preparation, morphology, and release kinetics. *J. Agric. Food Chem.* **2012**, *60* (16), 4111−4119.
(66) Shakiba, S.; Astete, C. E.; Paudel, S.; Sabliov, C. M.; Rodrigues, D. F.; Louie, S. M. Emerging investigator series: polymeric nanocarriers for agricultural applications: synthesis, characterization, and environmental and biological interactions. *Environ. Sci.: Nano* **2020**, *7* (1), 37−67.
(67) Kamble, S.; Agrawal, S.; Cherumukkil, S.; Sharma, V.; Jasra, R. V.; Munshi, P. Revisiting zeta potential, the key feature of interfacial phenomena, with applications and recent advancements. *ChemistrySelect* **2022**, *7* (1), No. e202103084.
(68) Moreno, A.; Sipponen, M. H. Overcoming Challenges of Lignin Nanoparticles: Expanding Opportunities for Scalable and Multifunctional Nanomaterials. *Acc. Chem. Res.* **2024**, *57* (14), 1918−1930.
(69) Carvalho, L. B.; Godoy, I. S.; Preisler, A. C.; de Freitas Proença, P. L.; Saraiva-Santos, T.; Verri, W. A.; Fraceto, L. F.; et al. Pre-emergence herbicidal efficiency and uptake of atrazine-loaded zein nanoparticles: a sustainable alternative to weed control. *Environ. Sci.: Nano* **2023**, *10* (6), 1629−1643.
(70) Grillo, R.; dos Santos, N. Z. P.; Maruyama, C. R.; Rosa, A. H.; de Lima, R.; Fraceto, L. F. Poly (ε-caprolactone) nanocapsules as carrier systems for herbicides: Physico-chemical characterization and genotoxicity evaluation. *J. Hazard. Mater.* **2012**, *231*−*232*, 1−9.
(71) Grillo, R.; Pereira, A. E.; Nishisaka, C. S.; de Lima, R.; Oehlke, K.; Greiner, R.; Fraceto, L. F. Chitosan/tripolyphosphate nanoparticles loaded with paraquat herbicide: an environmentally safer alternative for weed control. *J. Hazard. Mater.* **2014**, *278*, 163−171.
(72) Ge, M.; Li, Y.; Zhu, C.; Liang, G.; SM, J. A.; Hu, G.; Gui, Y.; M, J. R. Preparation of organic-modified magadiite−magnetic nanocomposite particles as an effective nanohybrid drug carrier material for cancer treatment and its properties of sustained release mechanism by Korsmeyer−Peppas kinetic model. *J. Mater. Sci.* **2021**, *56* (25), 14270−14286.
(73) Houston, R. W.; Elder, T. J.; Abdoulmoumine, N. H. Investigation into the pyrolysis bond dissociation enthalpies (BDEs) of a model lignin oligomer using density functional theory (DFT). *Energy Fuels* **2022**, *36* (3), 1565−1573.
(74) Sherard, M. M.; Dang, Q. M.; Reiff, S. C.; Simpson, J. H.; Leopold, M. C. On-site detection of neonicotinoid pesticides using functionalized gold nanoparticles and halogen bonding. *ACS Appl. Nano Mater.* **2023**, *6* (10), 8367−8381.
(75) Cheng, S.; Wang, J.; Yang, J.; Wang, X.; Tang, J. An effective strategy to design high-performance wide bandgap polymer donors for organic solar cells by increasing the backbone curvature. *Dyes Pigm.* **2023**, *219*, No. 111626.
(76) Hellal, A.; Abdelsalam, H.; Tawfik, W.; Ibrahim, M. A. Removal of Atrazine from contaminated water by functionalized graphene quantum dots. *Opt. Quantum Electron.* **2024**, *56* (3), 374.
(77) Hellal, A.; Abdelsalam, H.; Tawfik, W.; Ibrahim, M. A. Assessment of doped graphene in the removal of atrazine from water. *Sci. Rep.* **2024**, *14* (1), No. 21994.
(78) Liu, M.; Xiang, B.; Li, H.; He, X.; Li, H.; Du, K.; Li, X. A sustainable Poly (deep eutectic solvents) based molecular imprinting strategy with experimental and theoretical elucidation: Application for removal of atrazine in agricultural wastewater. *Sep. Purif. Technol.* **2025**, *353*, No. 128637.
(79) Hoffmann, G.; Chermette, H.; Morell, C. Revisiting nucleophilicity: an index for chemical reactivity from a CDFT approach. *J. Mol. Model.* **2024**, *30* (7), 232.
(80) Perveen, M.; Noreen, L.; Waqas, M.; Mehmood, R. F.; Iqbal, J.; Manzoor, S.; Khera, R. A.; et al. A DFT approach for finding therapeutic potential of graphyne as a nanocarrier in the doxorubicin drug delivery to treat cancer. *J. Mol. Graphics Modell.* **2023**, *124*, No. 108537.
(81) Pearson, R. G. The principle of maximum hardness. *Acc. Chem. Res.* **1993**, *26* (5), 250−255.
(82) Ben Haj Fraj, S.; Chaabene, M.; Agren, S.; El Haskouri, J.; Lahcini, M.; Ben Chaâbane, R.; Baouab, M. H. V. High incorporation of magnetite nanoparticles inside tetraaza macrocyclic Schiff base cavity: spectroscopic characterization and modeling by DFT calculation. *J. Iran. Chem. Soc.* **2022**, *19* (12), 4803−4822.
(83) Mirza, L. A.; Salih, R. O.; Abdullah, N. R. Calcite nanostructure as a novel drug carrier for 5-Fluorouracil chemotherapy agent: A computational study using DFT and AIMD. *Comput. Theor. Chem.* **2025**, *1248*, No. 115181.

(84) Bryant, M. T.; Ren, J.; Sharma, V. K.; Ma, X. Mutual Effects and Uptake of Organic Contaminants and Nanoplastics by Lettuce in Co-Exposure. *ACS Agric. Sci. Technol.* **2024**, *4* (4), 463−470.
(85) Zhang, H.; Xu, W.; Li, G.; Qu, H.; Ma, C.; Noruzi, E. B.; Li, H.; et al. Controlled release system of nanopesticides based on noncovalent interactions. *ACS Agric. Sci. Technol.* **2024**, *4* (9), 851−871.
(86) Parkinson, S. J.; Tungsirisurp, S.; Joshi, C.; Richmond, B. L.; Gifford, M. L.; Sikder, A.; Napier, R. M.; et al. Polymer Nanoparticles Pass the Plant Interface. *Nat. Commun.* **2022**, *13* (1), No. 7385.
(87) Hennig, T. B.; Bandeira, F. O.; Puerari, R. C.; Fraceto, L. F.; Matias, W. G. A systematic review of the toxic effects of a nanopesticide on non-target organisms: Estimation of protective concentrations using a species sensitivity distribution (SSD) approach−The case of atrazine. *Sci. Total Environ.* **2023**, *871*, No. 162094.
(88) Queiroz, A. M.; Pontes, M. S.; Scherer, M. D.; Graciano, D. E.; Caires, A. R.; Oliveira, S. L. Root Length as a Bioindicator of Pesticide Concentration in Irrigation Water. *Environ. Sci. Pollut. Res.* **2024**, *31* (59), 67140−67147.
(89) Zhang, J. J.; Yang, H. Metabolism and detoxification of pesticides in plants. *Sci. Total Environ.* **2021**, *790*, No. 148034.
(90) Lescano, M. R.; Macagno, J.; Berli, C. L. Model-Based Analysis of *Lactuca sativa* Root Growth under the Action of Herbicides in Milli-Channel Arrays with *In Situ* Imaging. *J. Agric. Food Chem.* **2023**, *71* (36), 13255−13262.
(91) Shahid, M.; Shafi, Z.; Ilyas, T.; Singh, U. B.; Pichtel, J. Crosstalk between Phytohormones and Pesticides: Insights into Unravelling the Crucial Roles of Plant Growth Regulators in Improving Crop Resilience to Pesticide Stress. *Sci. Hortic.* **2024**, *338*, No. 113663.
(92) Jiang, D.; Jiang, Z.; Liu, S.; Hu, Y.; Deng, S.; Wang, J.; Zhang, Y.; et al. Inhibition mechanism of atrazine on soybean growth insight from the plant nitrogen fixation and rhizobia diversity inhabiting in nodules and rhizosphere soil. *Appl. Soil Ecol.* **2024**, *195*, No. 105236.
(93) Ribeiro, C.; Stitt, M.; Hotta, C. T. How Stress Affects Your Budget—Stress Impacts on Starch Metabolism. *Front. Plant Sci.* **2022**, *13*, No. 774060.
(94) Jiang, D.; Li, Y.; Wang, J.; Lv, X.; Jiang, Z.; Cao, B.; Zhang, Y.; et al. Exogenous application of *Bradyrhizobium japonicum* AC20 enhances soybean tolerance to atrazine via regulating rhizosphere soil microbial community and amino acid, carbohydrate metabolism related genes expression. *Plant Physiol. Biochem.* **2023**, *196*, 472−483.
(95) Vieira, L. A.; Alves, R. D.; Menezes-Silva, P. E.; Mendonça, M. A.; Silva, M. L.; Silva, M. C.; Farnese, F. S.; et al. Water contamination with atrazine: is nitric oxide able to improve Pistia stratiotes phytoremediation capacity? *Environ. Pollut.* **2021**, *272*, No. 115971.
(96) Neto, F. A. N.; de Freitas Souza, M.; Blat, N. R.; da Silva, F. D.; Fernandes, B. C. C.; das Chagas, P. S. F.; Silva, D. V. Sensitivity and Antioxidant Response of Forest Species Seedlings to Atrazine under Simulated Conditions of Subsurface Water Contamination. *Chemosphere* **2024**, *360*, No. 142411.
(97) Del Buono, D.; Luzi, F.; Puglia, D. Lignin nanoparticles: A promising tool to improve maize physiological, biochemical, and chemical traits. *Nanomaterials* **2021**, *11* (4), 846.
(98) Swapnil, P.; Meena, M.; Singh, S. K.; Dhuldhaj, U. P.; Marwal, A. Vital roles of carotenoids in plants and humans to deteriorate stress with its structure, biosynthesis, metabolic engineering and functional aspects. *Curr. Plant Biol.* **2021**, *26*, No. 100203.
(99) Wang, D.; Saleh, N. B.; Byro, A.; Zepp, R.; Sahle-Demessie, E.; Luxton, T. P.; Su, C.; et al. Nano-enabled pesticides for sustainable agriculture and global food security. *Nat. Nanotechnol.* **2022**, *17* (4), 347−360.
(100) Jomova, K.; Raptova, R.; Alomar, S. Y.; Alwasel, S. H.; Nepovimova, E.; Kuca, K.; Valko, M. Reactive oxygen species, toxicity, oxidative stress, and antioxidants: Chronic diseases and aging. *Arch. Toxicol.* **2023**, *97* (10), 2499−2574.
(101) Taban, A.; Saharkhiz, M. J.; Khorram, M. Formulation and assessment of nano-encapsulated bioherbicides based on biopolymers and essential oil. *Ind. Crops Prod.* **2020**, *149*, No. 112348.
(102) Salinas, F.; Astete, C. E.; Waldvogel, J. H.; Navarro, S.; White, J. C.; Elmer, W.; Sabliov, C. M.; et al. Effects of Engineered Lignin-Graft-PLGA and Zein-Based Nanoparticles on Soybean Health. *NanoImpact* **2021**, *23*, No. 100329.
(103) Harper, A. R.; Dobson, R. C.; Morris, V. K.; Moggré, G. J. Fermentation of plant-based dairy alternatives by lactic acid bacteria. *Microb. Biotechnol.* **2022**, *15* (5), 1404−1421.
(104) Zhao, H.; Chen, H.; Zhao, B. Glycolic acid addition enhances lead uptake and transport by *Hydrangea macrophylla* (Thunb.) Ser. of different plant ages. *Environ. Technol. Innovation* **2024**, *36*, No. 103877.
(105) Munhoz-Garcia, G. V.; Takeshita, V.; de Oliveira, J. L.; Dalla Vecchia, B.; Nalin, D.; Pinácio, C. D. W.; Fraceto, L. F.; et al. Nanobased Natural Polymers as a Carrier System for Glyphosate: An Interesting Approach Aimed at Sustainable Agriculture. *J. Agric. Food Chem.* **2025**, *73*, 1097−1111, DOI: 10.1021/acs.jafc.4c08328.
(106) Pontes, M. S.; Antunes, D. R.; Oliveira, I. P.; Forini, M. M.; Santos, J. S.; Arruda, G. J.; Grillo, R.; et al. Chitosan/Tripolyphosphate Nanoformulation Carrying Paraquat: Insights on Its Enhanced Herbicidal Activity. *Environ. Sci.: Nano* **2021**, *8* (5), 1336−1351.
(107) Zhao, Y. W.; Wang, C. K.; Huang, X. Y.; Hu, D. G. Anthocyanin stability and degradation in plants. *Plant Signaling Behav.* **2021**, *16* (12), No. 1987767.
(108) Alscher, R. G.; Erturk, N.; Heath, L. S. Role of superoxide dismutases (SODs) in controlling oxidative stress in plants. *J. Exp. Bot.* **2002**, *53* (372), 1331−1341.
(109) Sobiecka, E.; Mroczkowska, M.; Olejnik, T. P. The Enzymatic Antioxidants Activities Changes in Water Plants Tissues Exposed to Chlorpyrifos Stress. *Antioxidants* **2022**, *11* (11), 2104.
(110) Niu, N. N.; Zhao, W. J.; Xiao, B. L.; Liang, Y. C.; Meng, X.; Song, X. Y.; Moosavi-Movahedi, A. A. Quench Treatment Cytochrome c: Transformation from a Classical Redox Protein to a Peroxidase Like Enzyme. *J. Iran. Chem. Soc.* **2022**, *19*, 2347−2357.
(111) De Oliveira, F. K.; Santos, L. O.; Buffon, J. G. Mechanism of action, sources, and application of peroxidases. *Food Res. Int.* **2021**, *143*, No. 110266.
(112) Di, X.; Fu, Y.; Xu, Y.; Zheng, S.; Huang, Q.; Sun, Y. Assessment of CuO NPs on soil microbial community structure based on phospholipid fatty acid techniques and phytotoxicity of bok choy seedlings. *Plant Physiol. Biochem.* **2023**, *197*, No. 107657.
(113) Zhang, Y.; Xu, J.; Li, R.; Ge, Y.; Li, Y.; Li, R. Plants' response to abiotic stress: Mechanisms and strategies. *Int. J. Mol. Sci.* **2023**, *24* (13), No. 10915.
(114) Zhao, J.; Lu, C.; Tariq, M.; Xiao, Q.; Zhang, W.; Huang, K.; Liu, Z.; et al. The response and tolerance mechanisms of lettuce (*Lactuca sativa* L.) exposed to nickel in a spiked soil system. *Chemosphere* **2019**, *222*, 399−406.
(115) An, J.; Hu, P.; Li, F.; Wu, H.; Shen, Y.; White, J. C.; Giraldo, J. P.; et al. Emerging investigator series: molecular mechanisms of plant salinity stress tolerance improvement by seed priming with cerium oxide nanoparticles. *Environ. Sci.: Nano* **2020**, *7* (8), 2214−2228.
(116) Simoni, S.; Castellacci, M.; Usai, G.; Rogo, U.; Mascagni, F.; Giordani, T.; Vangelisti, A.; et al. Genome-Wide Characterization of Class III Peroxidases and Their Expression Profile during Mycorrhizal Symbiosis and Phosphorus Deprivation in Lettuce (*Lactuca sativa* L.). *Horticulturae* **2024**, *10* (11), No. 1170.
(117) Zhou, J.; Hu, Q.; Xiao, X.; Yao, D.; Ge, S.; Ye, J.; Xing, W.; et al. Mechanism of phosphate sensing and signaling revealed by rice SPX1-PHR2 complex structure. *Nat. Commun.* **2021**, *12* (1), No. 7040.
(118) Ramel, F.; Sulmon, C.; Bogard, M.; Couée, I.; Gouesbet, G. Differential Patterns of Reactive Oxygen Species and Antioxidative Mechanisms during Atrazine Injury and Sucrose-Induced Tolerance in *Arabidopsis thaliana* Plantlets. *BMC Plant Biol.* **2009**, *9*, No. 28.
(119) Zhang, Y.; Li, Z.; Zhang, N.; Chai, X. The effects of FR and UVA irradiation timing on multi-omics of purple lettuce in plant factories. *Agriculture* **2024**, *14* (11), No. 2019.

(120) Wang, Y.; Ma, X.; Shang, W.; Luo, H.; Wang, L.; Sun, K.; Zhang, T.; et al. Comparative transcriptome analysis reveals differential mechanisms of soft rot resistance in lettuce grown under white and blue light. *Food Energy Secur.* **2025**, *14* (1), No. e70038.
(121) Kolahi, M.; Kazemi, E. M.; Yazdi, M.; Goldson-Barnaby, A. Oxidative stress induced by cadmium in lettuce (*Lactuca sativa* Linn.): Oxidative stress indicators and prediction of their genes. *Plant Physiol. Biochem.* **2020**, *146*, 71−89.
(122) Tripathi, D.; Singh, M.; Pandey-Rai, S. Crosstalk of nanoparticles and phytohormones regulate plant growth and metabolism under abiotic and biotic stress. *Plant Stress* **2022**, *6*, No. 100107.
(123) Weng, Y.; Bai, X.; Kang, M.; Ji, Y.; Wang, H.; Liu, Y. Detoxification strategy of titanium oxide nanoparticles driving endogenous molecules metabolism to modulate atrazine conversion in *Lactuca sativa* L. *Environ. Sci. Technol.* **2025**, *59* (13), 6440−6451.
(124) Cheng, B.; Ding, Z.; Yue, L.; Chen, F.; Cao, X.; Li, J.; Wang, Z.; Wang, Z. Carbon dots enhanced cold tolerance of lettuce (*Lactuca sativa* L.): scavenging reactive oxygen species, modulating hormones and up-regulating gene expression. *Environ. Sci.: Nano* **2023**, *10* (10), 2849−2860.
(125) Gupta, S. D.; Agarwal, A.; Pradhan, S. Phytostimulatory effect of silver nanoparticles (AgNPs) on rice seedling growth: An insight from antioxidative enzyme activities and gene expression patterns. *Ecotoxicol. Environ. Saf.* **2018**, *161*, 624−633.
(126) Javaid, M. H.; Chen, N.; Yasin, M. U.; Fan, X.; Neelam, A.; Rehman, M.; Gan, Y.; et al. Green-synthesized lignin nanoparticles enhance Zea mays resilience to salt stress by improving antioxidant metabolism and mitigating ultrastructural damage. *Chemosphere* **2024**, *359*, No. 142337.
(127) Chang, J.; Gao, K.; Li, R.; Dong, F.; Zheng, Y.; Zhang, Q.; Li, Y. Comparative uptake, translocation and metabolism of phenamacril in crops under hydroponic and soil cultivation conditions. *Sci. Total Environ.* **2024**, *925*, No. 171670.
(128) Gomes, S. I.; Scott-Fordsmand, J. J.; Campos, E. V.; Grillo, R.; Fraceto, L. F.; Amorim, M. J. On the safety of nanoformulations to non-target soil invertebrates−an atrazine case study. *Environ. Sci.: Nano* **2019**, *6* (6), 1950−1958.
(129) Chikoye, D.; Udensi, U. E.; Lum, A. F. Evaluation of a new formulation of atrazine and metolachlor mixture for weed control in maize in Nigeria. *Crop Prot.* **2005**, *24* (11), 1016−1020.
(130) Jalal, A.; de Oliveira Junior, J. C.; Ribeiro, J. S.; Fernandes, G. C.; Mariano, G. G.; Trindade, V. D. R.; Dos Reis, A. R. Hormesis in plants: Physiological and biochemical responses. *Ecotoxicol. Environ. Saf.* **2021**, *207*, No. 111225.
(131) Khamare, Y.; Marble, S. C.; Pearson, B. J.; Chen, J.; Devkota, P. Effect of weed competition on growth of container grown ornamentals plants in four different container sizes. *Horticulturae* **2023**, *9* (3), No. 317.
(132) Andriana, Y.; Xuan, T. D. Contribution of phenolic acids and dimethyl sulfone to the allelopathic effect of invasive *Tridax procumbens*. *Pesqui. Agropecu. Trop.* **2020**, *50*, No. e64792.
(133) Qi, Y.; Li, J.; Fu, G.; Zhao, C.; Guan, X.; Yan, B.; Ren, M. Effects of Sublethal Herbicides on Offspring Germination and Seedling Growth: Redroot Pigweed (*Amaranthus retroflexus*) vs. Velvetleaf (*Abutilon theophrasti*). *Sci. Total Environ.* **2018**, *645*, 543−549.
(134) Takeshita, V.; de Sousa, B. T.; Preisler, A. C.; Carvalho, L. B.; Santo Pereira, A. D. E.; Tornisielo, V. L.; Fraceto, L. F.; et al. Foliar absorption and field herbicidal studies of atrazine-loaded polymeric nanoparticles. *J. Hazard. Mater.* **2021**, *418*, No. 126350.
(135) Sousa, G. F. M.; Gomes, D. G.; Campos, E. V.; Oliveira, J. L.; Fraceto, L. F.; Stolf-Moreira, R.; Oliveira, H. C. Post-Emergence Herbicidal Activity of Nanoatrazine against Susceptible Weeds. *Front. Environ. Sci.* **2018**, *6*, No. 12.
(136) Dong, J.; Liu, X.; Chen, Y.; Yang, W.; Du, X. User-safe and efficient chitosan-gated porous carbon nanopesticides and nano-herbicides. *J. Colloid Interface Sci.* **2021**, *594*, 20−34.
(137) Restu, W. K.; Septiyanti, M.; Triwulandari, E.; Aryana, N.; Sampora, Y.; Devy, Y. A.; Ogino, C.; et al. The Preparation of Nanoemulsion Formulation from Pelargonic Acid in Lignin Carrier and Its Application to Weeds. *J. Inst. Eng. (India): Ser. E* **2023**, *104* (2), 297−303.
(138) Restu, W. K.; Aryana, N.; Septiyanti, M.; Triwulandari, E.; Sampora, Y.; Devy, Y. A.; Ogino, C.; et al. Development of a Lignin-Based Carrier-Citronella Oil Nanoemulsion and Its Utilization as an Herbicide against Specific Weed Species. *Chem. Biodiversity* **2024**, *21* (9), No. e202400861.

https://doi.org/10.1021/acssuschemeng.5c05651
ACS Sustainable Chem. Eng. 2025, 13, 15460−15477